Compatibilizing action of a poly(styrene-butadiene) triblock copolymer in ABS/PET-G blends

SUSAN JOSEPH[1]*, WALTER W. FOCKE[1], SABU THOMAS[2]

[1]*Institute of Applied Materials, Department of Chemical Engineering, University of Pretoria, South Africa*

[2]*School of Chemical Sciences, Mahatma Gandhi University, Priyadarshini Hills, P. O. Kottayam, Kerala, India 686560*

*Corresponding author:

Fax: +27- 12- 420 2516

Tel: +91 -12 -4203728 (off)

E-mail address: susanaruvi@gmail.com

Abstract—The morphology of blends of poly(acrylonitrile-co-butadiene-co-styrene) (ABS) and poly (ethylene terephthalate glycol (PET-G) has been investigated with special reference to the effect of blend ratio and compatibilization. Scanning electron microscopy (SEM) examination revealed different morphologies such as dispersed, cocontinuous and phase inverted depending on the composition, indicating that the binary blends are immiscible and forms a two-phase structure. Tensile properties decreased with increase in the ABS content while the impact strength reached an optimum at ca. 70% ABS. Influence of a triblock copolymer based on styrene and butadiene (SBS) on morphology, mechanical measurements and failure topography was used as criteria of the compatibilization effect. The compatiblizing action of SBS was evidenced by the sharp decrease in domain size of the dispersed phase followed by an increase at higher concentrations. The conformation of the compatibilizer at the interface was further analyzed based on the area occupied by the compatibilizer at the blend interface. The results were in agreement with the theoretical predictions of Noolandi and Hong. The extent of interface adhesion in these blends was analyzed by examination of the fracture-surface morphology. Addition of SBS also improved notched impact, elongation-at-break, tensile strength and modulus of elasticity. These results confirm that SBS is an effective compatibilizer for ABS/PET-G blends.

Keywords: Polymer blends; compatibilization; mechanical properties; morphology; ABS; PET-G.

1. INTRODUCTION

Advanced materials with desired properties are increasingly developed by blending commodity polymers. In industry, this process is mainly realized by means of extrusion-compounding of the component polymers. Normally the end-products obtained in this manner exhibit complicated phase morphologies. This is due to the fact that polymers of different chemical nature are in the general case sparingly soluble in each other and that they become finely dispersed in the flow fields during processing. Many industrially important polymer systems are multiphase in nature and are often stabilized through the addition of compatibilizing or dispersing agents. These agents are usually copolymers and may be generated in-situ by reaction of the blend components. The phase structure is of central importance for the mechanical properties of polymer blends. The work required to produce new contact surface areas between the coexisting phases has been studied intensely [1-2]. It is one of the most important parameters determining the degree of subdivision and the action of interfacial modifiers or compatibilizers. Block or graft copolymers with the same or similar structure to the blend components are suitable for physical compatibilization. A compatibilizer comprising two parts, each miscible or compatible with one of the polymers tends to locate itself at the interface. This improves interfacial adhesion and reduces the interfacial tension between the phases allowing the achievement of finer dispersion of the phases (emulsification effect) [3]. This is advantageous as impact toughness usually is the mechanical property that suffers the most from blend incompatibility.

Several patents consider blends based on poly(ethylene terephthalate (PET) [4-7], and poly(acrylonitrile-co-butadiene-co-styrene)(ABS) [8-13]. Recently, Xue *et al.* [14] studied miscibility and compatibilization of poly(trimethylene terephthalate)/poly(acrylonitrile-butadiene-styrene) blends. PET-based blends have received increasing commercial attention owing to their physical and mechanical properties. Paul and co-workers [11] characterized the fracture behaviour of PC/ABS/SAN blends. Mamat *et al.* [12] compared deformation mechanisms during fracture of nylon-6/ABS blends, both neat and modified with an imidized acrylic polymer. They concluded that the compatibilized blends failed by cavitations at the rubber particles followed by massive shear yielding of the PA matrix. The mechanical properties (impact strength, tensile properties) of poly(ethylene terephthalate) (PET) and its blends with acrylonitrile-butadiene-styrene (ABS) copolymers were found to dependent on processing conditions [13].

ABS is a tough non polar thermoplastic styrene polymer. It is a multi-phase material in which rubber particles are embedded in a poly(styrene-co-acrylonitrile) matrix. In ABS,

acrylonitrile imparts chemical resistance and weatherability; butadiene provides the rubber toughness character, and styrene gives glossiness and processability. The compositions of the various components in ABS can be controlled to meet the requirements of a variety of applications.

Polyesters represent an important class of engineering thermoplastics that find many applications. However, they are brittle and have low impact strength. In PET-G, the "G" represents the cyclohexane dimethanol modifier. It is incorporated to reduce brittleness and limit the premature aging characteristic of unmodified amorphous poly(ethylene terephthalate). The ABS/PET-G blends combine good toughness with excellent processability. However, they are highly immiscible and incompatible due to the high polarity difference between the component polymers. Styrene butadiene styrene rubber (SBS) is the impact modifiers of interest. It features a hard-soft-hard triblock sequence in which the continuous soft rubber phase is formed by the inner block consisting of randomized poly(styrene-co-butadiene). It was chosen on the basis of structural considerations, its low density, and low molecular weight and the fact that it is physically compatible with both ABS and PET.

The aim of this investigation was to perform a systematic study on the morphology and mechanical properties of ABS/PET-G blends in the presence and absence of SBS. Blends of ABS and PET-G are highly incompatible and show macrophase separation. Addition of the copolymer is expected to decrease the degree of phase separation and reduce the size of the dispersed phase domains. In the present paper, scanning electron microscopy was used to characterise the dimensions of the dispersed phase in the presence and absence of the copolymer compatibilizer. The effect of compatibilization on morphological parameters such as domain size, interfacial area per unit volume and the interparticle distance of dispersed droplets was studied in detail. The mechanical properties of these blends were correlated with the microstructure of the blends. Failure surface topography was studied in order to gain more insight on the dependence of the blend structure on the copolymer addition. The conformation of the compatibilizer at the interface was deduced from the area occupied by the compatibilizer molecules at the interface. Finally, attempts were made to correlate the mechanical properties with the microstructure of the blends.

2. EXPERIMENTAL

2.1. Materials

ABS is a graft copolymer with 38 wt. % nitrile rubber (butadiene:acrylonitrile = 93.7:6.3) and styrene acrylonitrile copolymer, (styrene:acrylonitrile = 73:27). Poly(ethylene terephthalate-co-cyclohexane dimethanol terephthalate) or PET-G is water-clear amorphous thermoplastic copolyester with a glass transition temperature of ca. 80°C. The compatibilizer used is SBS, a copolymer of styrene (65 %) with butadiene (35 %) blocks. The key properties of the materials used in this work are presented in Table 1.

Table 1.

Selected properties of the polymers and their suppliers

Item	Description / Grade	Density kg/m^3	MFR dg/min	Supplier
ABS	MA-221	1030	5.5 [a]	BASF
PET-G	Spectar 14471	1270	-	Eastman
SBS	Styroflex 2G66	998	13 [b]	BASF

[a] 220°C/10 kg; [b] 200°C/5 kg

2.2. Blend preparation

The polymeric materials were dried in a dehumidifying drier at 80°C for 12 hours before melt processing at 220°C to ensure complete removal of sorbed water. Blends were prepared from premixed polymer pellets in a 25 mm, 30 L/D Rapra single screw extruder. The screw speed was set at 65 rpm and the temperature profile was set: 210/220/220/220°C. The extruded strands were pelletized and dried before injection molding into ASTM tensile test specimens on an Engel injection-moulder.

2.3. Mechanical properties

Tensile tests were conducted at room temperature on a Zwick 1456 tensile tester using the ISO 527-2/1A/50 protocol, i.e. at a draw speed of 50 mm/min. Notched Charpy impact properties were determined on a Zwick impact tester using the ISO179/1eA protocol. A V-shaped single edge notched was cut after injection moulding (2 mm depth, 45° angle and notch tip radius 0. 25 mm). For each data point, the mean values listed were based on at least five replicated measurements for tensile and eight for impact tests.

2.4. Phase morphology studies

Scanning electron microscopy (SEM) observations were conducted on a JSM-840 J scanning electron microscope using an acceleration voltage at 20 kV. For better insight into the blend morphology, the specimens for morphology studies were cryogenically fractured and then extracted with suitable solvents. In ABS rich blends, the dispersed PET-G phase was etched with 10% KOH in ethanol at ambient temperature for 24 hours. In PET-G rich blends 2-butanone was used to preferentially extract (for 24 h) the dispersed ABS phase. The etched surface was dried and then sputter coated with a fine gold layer to provide proper surface conduction. Photographs were taken at different fields of view and at different magnifications. About 400 particles were considered to determine the droplet diameter of the dispersed phase using image analysis software. The photographs were quantitatively analyzed in terms of different number average and "weight" average domain diameters respectively defined as follows [15]:

Number-average domain diameter: $$\overline{D}_n = \frac{\sum N_i D_i}{\sum N_i} \quad (1)$$

"Weight"-average domain diameter: $$\overline{D}_w = \frac{\sum N_i D_i^2}{\sum N_i D_i} \quad (2)$$

In these equations, N_i is the number of domains having diameter D_i. The morphological parameters of polydispersity index (PDI) [16], interfacial area per unit volume and interparticle distance (IPD) [17] for the dispersed droplets were estimated as follows:

Polydispersity index: $$PDI = \frac{\overline{D}_w}{\overline{D}_n} \quad (3)$$

Interfacial area per unit volume: $$a = 6\phi / D_n \quad (4)$$

Interparticle distance: $$IPD = D_n \left[\left(\frac{\pi}{6\phi} \right)^{1/3} - 1 \right] \quad (5)$$

where ϕ is the volume fraction of the dispersed phase.

2.5 Fractography

The images of the specimen after the impact test are recorded by using a JSM-840 J scanning electron microscope using an acceleration voltage at 20 kV.

3. RESULTS AND DISCUSSION

3.1. Morphology of the neat blend

At fixed processing conditions and blend composition the morphology is determined by the shear rate during mixing, the interfacial tension and the viscosity ratios of the components. The morphology of a blend strongly influences its ultimate properties. Fig. 1 (a)-(g) shows the scanning electron micrographs of the 10/90, 30/70, 40/60, 50/50, 60/40, 70/30 and 90/10 ABS/PET-G blends. PET has a higher electron density and is indicated by the darker regions. The lightly shaded domains seen in the ABS regions are attributed to the SAN phase as it has a lower electron density. The holes in the Figs. 1 (a) and (b) indicate the ABS phase domains that have been etched away by the solvent. The morphology of the 10/90, 30/70 of the ABS/PET-G blends show a two phase structure in which the minor ABS phase is dispersed as discrete domains in the continuous PET-G matrix. As the proportion of ABS in the blend increases, the dispersed phase domain size steadily increases from 2.48 μm in ABS/PET-G (10/90) to 3.76 μm in ABS/PET-G (30/70). Co-continuous morphologies, with dispersed and semi-continuous phases, are observed at 40/60, 50/50 and 60/40 ABS/PET-G compositions (Figs. 1(c), (d) and (e)). It was reported [18] that ABS-containing blends that show a yield stress feature stable co-continuous structures over a broad composition range. This is followed by a phase inversion beyond 60 wt. % of ABS as observed in other blend systems [19-20]. The domain diameters calculated according to equations (1) to (2) from micrographs of the present samples, as well as the polydispersity indices values calculated according to equation (3), also supports this observation. See Table 2.

Table 2.

Domain size, interparticle distance and interfacial area measurements of ABS/PET-G blends

Ratio ABS/PET-G	$\overline{D}_n$ (μm)	$\overline{D}w$ (μm)	PDI	IPD (μm)	Interfacial area/unit volume ($\mu m^2/\mu m^3$)
10/90	2.48	3.10	1.25	1.13	0.288
30/70	3.76	5.48	1.46	1.86	0.550
70/30	3.18	4.36	1.37	1.05	0.487
90/10	2.08	2.25	1.08	2.29	0.237

Blends of ABS dispersed in PET-G showed larger dispersed particle sizes than the blend of PET-G dispersed in ABS at comparable compositions (Fig. 2). The phenomenon of coalescence is more pronounced at high concentration of the dispersed ABS phase. The high

mobility of ABS domains in the low viscosity PET-G matrix is responsible for the high extent of coalescence phenomenon of rubber domains. This phenomenon was reported by several authors [21-22]. As a result, the equilibrium between domain break-up and coalescence is shifted more in the direction of coalescence in blends where ABS is dispersed in PET-G. Thus deformation of the two colliding drops is lower at higher dispersed phase viscosities. It is interesting to compare the interfacial area at 30% of the dispersed phase concentration of the PET-G and ABS phase. When PET-G is the dispersed phase the interfacial area is high due to its smaller size on account of less coalescence. The area of contact of smaller dispersed particles with the matrix is larger than bigger particles, giving rise to better interfacial adhesion. The reverse trend of domain size is seen for interparticle distance. In short, all morphological parameters confirm that the blends are highly incompatible with non-uniform and coarse phase morphology.

3.2 Phase morphology of compatibilized blends

Incompatible blends are characterized by a two-phase morphology, a thin interphase region, and weak physical and chemical interactions across the phase boundaries. The ABS/PET-G (70/30) blends with and without compatibilizer were observed with SEM to study the effect of emulsifying agent on the phase morphology. Figs. 3 (a-d) shows the morphology of the ABS/PET-G (70/30) blends containing 1, 3, 5 and 10 wt. % SBS respectively. The neat blend contains more large particles as seen in Fig. 1(f). Fig. 3 (a) shows PET-G particles uniformly dispersed within ABS matrix. The compatibilized blends yield significantly smaller particles than the neat blend. The morphology of the compatibilized blends shows that the addition of the block copolymer results in a considerable reduction in the dispersed domain size. The dispersion was observed to be more homogenous and finer. At this point, the compatibilizer occupies the maximum interfacial area. The final domain size is determined by the balance between the shear force that causes droplet break-up, and interfacial tension that counteracts droplet deformation and coalescence. Thus, addition of compatibilizer beyond the saturation point does not result in any further decrease in D_n. The results are expected in the present investigation as the compatibilizer, SBS, plays the role of an emulsifier that prevent particle coalescence and increases the interfacial adhesion between the ABS and PET-G phases. The butadiene part interacts with PET-G phase, while the styrene part is miscible with styrene-acrylonitrile phase of ABS [23]. The copolymers diffuse to the interface formed between the homopolymers, forming shells around the dispersed drops, thus reducing the interfacial tension and coalescence behaviour. Excessive copolymer addition simply leads to formation

of micelles instead of creating additional polymer-polymer interface. The mechanism of copolymer action at the interface is believed to be due to: (i) a reduction in the average size of the dispersed phase due to the suppression of coalescence and the decrease of interfacial tension, (ii) an increase in the break-up of the largest particles in the size distribution of the dispersed phase and a decrease of the mobility of the interface which slows down the coalescence rate.

A plot of the average domain diameter versus compatibilizer concentration is presented in Fig. 4. It shows that SBS has a significant effect on the ABS/PET-G phase morphology causing a considerable reduction in the domain size. The average domain size of the 70/30 ABS/PET-G binary blend is 3.18 μm. A 25% reduction in the domain size is observed on addition of only one wt. % SBS. A further increase in copolymer content has no appreciable effect with respect to domain size reduction. Thus there is an initial sharp decrease in dispersed phase particle size followed by a plateau region as the compatilizer content is increased. The morphology size reduction, induced by the addition of the copolymer, implies a stabilization of the blend morphology. It is attributed to two major effects (i) decrease of interfacial tension and (ii) suppression of coalescence of impinging droplets during the mixing process. One can invoke Taylor's theory [24] to explain the observed interfacial saturation point as a consequence of the mixing conditions. Taylor considers how the balance of applied shear forces and counteracting interfacial forces affects droplet dimensions and stability in a shear field. The equilibrium domain size is expressed in terms of the Weber number. It is only a function of the dispersed to continuous phase viscosity ratio at the mixing conditions. The Weber number is defined as follows:

$$We = \frac{\dot{\gamma}\,\eta_c D_n}{\Gamma} \tag{6}$$

where $\dot{\gamma}$ is the shear rate, η_c is the continuous phase melt viscosity, D_n is the equilibrium dispersed phase droplet size, and Γ is the interfacial tension between the two components. Addition of the compatibilizer decreases the interfacial tension and therefore aids liquid droplet deformation and breakdown. According to equation (6), droplet reduction is enhanced by large shear rates, a high continuous phase (matrix) melt viscosity and a low interfacial tension. This can be achieved by mixing at lower temperatures (higher viscosity of the continuous phase) or at higher screw speeds (increased $\dot{\gamma}$). The levelling off point observed in the plot of domain size versus compatibilizer content can be considered as an apparent critical micelle concentration (CMC) of the copolymer. Beyond this concentration the interfacial

tension remains constant and unaffected by further addition of the SBS. The localisation of the copolymer also results in a decrease in entropy and ultimately limits the amount of copolymer required at the interface. The separation of the two blocks into corresponding homopolymer phases leads to a decrease in the interaction energy of the oriented block with the homopolymers and a small decrease in entropy. The interfacial activity of the compatibilizer provides for better dispersion of the constituents and greater stability against recombination of the dispersed phase domains during mixing. The incorporation of more than 1% copolymer may considered to be wasteful, since the system has already achieved interfacial saturation, and further addition just leads to formation of micelles in the bulk polymer phases.

The various domain diameters, polydispersity index, interparticle distance and interfacial area measurements are presented in Table 3. The neat (70/30) blend of ABS/PET-G has an average domain size of 3.18 μm. Addition of 1% of block copolymer decreased the domain size to 2.38 μm, i.e. a 25% reduction in size occurs. Thus compatibilization stabilised the morphology by reducing the particle size, polydispersity index, interparticle distance, enhancing the interfacial area and interface adhesion. A critical concentration of compatibilizer required for effective compatibilization (CMC) was observed beyond which, there was no net improvement in interparticle properties and was considered as the point of interfacial saturation.

The area occupied by the block copolymer at the blend interface, Σ, was calculated using the expression suggested by Paul *et al.* [25]

$$\Sigma = \frac{3\phi_A M}{mrN} \tag{7}$$

where M is the molecular weight of the copolymer, N is the Avogadro number, ϕ_A is the volume fraction of the homopolymer A in the A/B blend, r the radius of the dispersed phase domains and m is the mass of copolymer required to saturate a unit volume of the blend interface (CMC). The conformation of copolymer at the blend interface can be inferred on the basis of the Σ value. Equation (7) establishes a direct link between the interfacial area and the dispersed phase domain size. As expected, the interfacial area increases up to the apparent CMC value and then levels off. At 1% SBS copolymer the maximum interfacial area has been attained.

Table 3.

Domain size, interparticle distance and interfacial area values for (70/30) ABS/PET-G blends

Concentration SBS (wt. %)	$\overline{D}_n$ (μm)	$\overline{D}w$ (μm)	PDI	IPD (μm)	Interfacial area/unit volume ($\mu m^2/\mu m^3$)
0	3.18	4.36	1.37	1.05	0.487
1	2.38	2.71	1.14	0.74	0.643
3	2.40	2.78	1.16	0.76	0.624
5	2.40	2.79	1.16	0.77	0.623

3.3. Comparison of the experimental compatibilization data with theory

Leibler [26] developed a thermodynamic theory for the emulsifying effect of a copolymer in a heterogeneous, semi-compatible polymer blend. According to this, the reduction in interfacial tension is due to the adsorption of copolymer at the interface. Noolandi and Hong [27-28] developed obtained an expression for the reduction in interfacial tension in highly incompatible blends. Their theory states that localization of some of the block copolymers at the interface causes a lowering of the interaction energy between the two immiscible homopolymers, broadens the interface between the homopolymers and decreases the free energy. The localisation of the copolymer also results in a decrease in entropy and ultimately limits the amount of copolymer required at the interface. The separation of the two blocks into corresponding homopolymer phases leads to a decrease in the interaction energy of the oriented blocks with the homopolymers and a small decrease in entropy. In essence though, it is the surface activity of the block copolymer chains that causes the interfacial tension reduction.

The Noolandi and Hong theory can be applied to incompatible systems such as ABS/PET-G for concentrations below the CMC. The reduction in interfacial tension ($\Delta\gamma$) in a heterogeneous binary A/B blend upon the addition of an A-B block copolymer is [28]:

$$\Delta\gamma = \frac{d\phi_c}{z_c}\left[0.5Z_c\chi + 1 - \exp\left(\frac{z_c\chi}{2}\right)\right] \quad (8)$$

where d is the width at half-height of the copolymer profile reduced by Kuhn statistical segment length, ϕ_c is the bulk copolymer volume fraction in the system, χ is the Flory Huggins interaction parameter and z_c is the degree of polymerisation of the copolymer. As mentioned, this theory is applicable to completely incompatible systems having concentration less than the CMC. However, above CMC, $\Delta\gamma$ levels off with ϕ_c but below CMC the plot of interfacial tension reduction versus ϕ_c should yield a straight line. Equation (8) shows that the interfacial tension reduction shows an exponential dependence on the block molecular weight. The reduction is also proportional to the homopolymer volume fraction. Thus it predicts that large molar mass diblock copolymers surfactants should be most effectiveness as

compatibilizers for immiscible homopolymers. Noolandi and Hong [28] pointed out that both copolymer concentration and molecular weight are important in reducing the interfacial tension. However, it is again stressed that their theoretical treatment is applicable only for concentrations well below the critical micelle concentration. Above the critical concentration, the compatibilizer does not enhance surface activity any further as it forms compatibilizer micelles in the continuous phase. Since the interfacial tension reduction is directly proportional to the particle size reduction at low volume fractions, Wu [17] argued that

$$\Delta D = K \frac{d\phi_c}{z_c}\left[0.5 Z_c \chi + 1 - \exp\left(\frac{z_c \chi}{2}\right)\right] \tag{9}$$

where ΔD is the particle size reduction or increment upon the addition of compatibilizer and K is a proportionality constant.

Fig. 5 plots the domain size reduction of the ABS/PET-G (70/30) blends as a function of SBS volume fraction. It can be noticed that at low concentration of the copolymer, ΔD decreases linearly with copolymer content and at high concentration, ΔD levels off. The reduction in domain size is due to the decrease in the interaction energy between homopolymers by the localization of the copolymer in the interfacial area. The interfacial activity of the copolymer decreases the interaction energy and hence the domain size. This is in agreement with the predictions of Noolandi and Hong [28].

3.4. Conformation of the compatibilizer at the interface

Fig. 6 depicts the three different physical models representing the conformation of a copolymer at blend interface. In the first model, the blocks of the copolymer extend to the corresponding homopolymer phase as shown in Fig. 6(a). In the second model the copolymer is believed to lie almost completely flat at the interface [Fig. 6 (b)]. The actual position can be represented by the model shown schematically in Fig. 6(c). A comparison of the experimental and calculated values of the interfacial area provides an indication of the actual conformation of the copolymer at the blend interface. The magnitude of the interfacial area of the compatibilizer at the blend interface at CMC was calculated as 14.8 nm^2. This value is intermediate between the fully extended model (0.5nm^2) and the flat model (106 nm^2). This suggests that the actual conformation of the copolymer at the domain interface is neither fully extended nor completely flat. In this model, a portion of the block copolymer remains at the interface and the rest penetrates into the corresponding homopolymer phases. This is in agreement with the model suggested by Thomas and Prud'homme [29].

3.5. Mechanical properties of binary blends

The mechanical properties of the ABS, PET-G and ABS/PET-G blends are reported in Table 4. The tensile properties measured include tensile strength at yield, the modulus of elasticity and the ductility (measured as the percentage elongation at break). The impact test provides a measure of the toughness of the material. In studying immiscible blends of rubbers and polymers, an increase in impact strength is usually paralleled by a significant decrease in both elastic modulus and yield stress. Tensile strength increases with the incorporation of PET-G into ABS. A sharp increase in tensile strength is observed when the PET-G content exceeds 50 wt. percent. This sharp increase in tensile strength is associated with the predominance of PET-G phase as the continuous phase. The trend is the same with percent elongation of the blends but the Young's modulus values varied little with composition. The elongation at break, a sensitive indicator of phase adhesion in polymer alloys, is drastically reduced at higher ABS contents. This could be due to the essentially incompatible nature of the blends. The inferior mechanical properties in binary blends are due to poor interfacial adhesion and bigger particle size of the dispersed phase. Note that the ABS grade used here is a high impact grade.

Table 4.

Mechanical properties of ABS/PET-G blends

ABS /PET-G ratio	Tensile strength (MPa)	Young's modulus (GPa)	Elongation at break (%)	Charpy notched impact (kJ/m^2)
0/100	49.5	0.70	47	1.3
10/90	48.7	0.70	43	2.2
25/75	46.4	0.61	37	3.7
40/60	29.7	0.65	44	8.1
50/50	41.5	0.67	22	8.8
60/40	39.1	0.70	20	13.0
65/35	38.9	0.64	18	18.8.
70/30	38.9	0.64	19	24.6
75/25	38.8	0.66	23	21.6
80/20	36.3	0.63	14	16.9
85/15	35.3	0.63	14	17.5
90/10	34.3	0.63	20	19.9
100/0	35.2	0.66	22	21.5

Adding PET-G to the ABS initially caused a decrease in the notched Charpy impact strength but the highest value is observed at intermediate levels of ca. 70 wt. % ABS. (Fig. 7). This improvement in the value of impact fracture energy coincides with a brittle–ductile transition in the mechanism of fracture. Similar reports on the mechanical properties of polymer blends have already been made in literature [11-13]. Suarez *et al.* [30] described the influence of the tensile strength contribution and the extent of elongation on mechanisms explaining the impact failure of rubber-modified plastics. The tensile strength increased in an almost linear fashion as the weight fraction of PET in the blend was increased. There was only a small difference in elongation at break (%) among the blends. In contrast, the notched Izod impact strength passed through a maximum at ca. 70 wt % PET. The current blends reported here exhibit synergism with respect to the impact strength: Values for the ABS-rich-blends are higher than expected from a weighted linear average of the component properties. It is known that particle agglomeration greatly reduces the toughening efficiency of rubber and that fine dispersion of particles is a prerequisite for toughening. In the present case, ABS/PET-G (70/30) blend has the highest impact strength, and its SEM indicates that there is a fine dispersion of rubber particles in the matrix.

3.6. Mechanical properties of compatibilized blends

The mechanical properties of the 70/30 ABS/PET-G blend with compatibilizer addition are summarized in Table 5 and the effect of copolymer on tensile and impact strength of 70/30 ABS/PET-G blend is demonstrated in Fig. 8. The neat 70/30 ABS/PET-G blend has a relatively low tensile strength. This can be explained by the poor stress transfer between the phases of the immiscible blends, resulting from the large dispersed particles having poor interfacial adhesion. Adding just 1 wt. % of the copolymer, SBS, improves tensile strength by 29%, above which, no further increase was observed up to 15 wt. %. The smaller the dispersed PET-G particles, the higher are the E_b values. The elongation at break increased by nearly 20 fold on adding 1 wt. % copolymer. Surprisingly, modulus increased nearly four times with a 1% compatibilizer dosage. The results of the Charpy notched impact results in Table 5 show a spectacular increase (64%) for the compatibilized blends over the incompatible counterpart. The marked increase in the mechanical properties for the compatibilized blend is attributed to the finer and homogenous dispersion, improved adhesion between the phases and a well developed interlayer formed by the compatibilizer.

Table 5.

Mechanical properties of compatibilized ABS/PET-G (70/30) blends

Wt. % compatiblizer	Tensile strength (MPa)	Young's modulus (GPa)	Elongation at break (%)	Charpy notched impact strength (kJ/m^2)
0	38.9	0.64	19	24.6
1	44.8	2.59	347	40.3
3	42.9	3.15	339	24.4
5	42.6	3.45	332	19.5
10	38.2	4.40	315	9.95
15	33.4	4.36	298	7.6

The compatibilizing action of SBS is due to the ability of butadiene part interacting with PET phase and the styrene part with ABS phase. A superior mechanical property (impact strength) was observed on ABS/PET-G/SBS blend at 1% copolymer addition. It is known that particle agglomeration greatly reduces the toughening efficiency of rubber and that fine dispersion of particles is a prerequisite for toughening. The improvement of the interfacial adhesion due to localization of the copolymer at the interface could provide an explanation for the improved properties of elongation at break and impact strength of the compatibilized blends. The presence of a third phase SBS (1%) enabled optimum stress transfer at the interface thus enhancing the properties of these blends [31-32]. Echevarría *et al.* [34] report similar observations for poly (trimethylene terephthalate)/poly(ethylene-co-octene) blends and Cho *et al.* [35] for rubber-modified poly(methyl methacrylate) blends.

3.7. Failure topography and extent of interface adhesion in binary blends

For promoting polymer blends for wider applications, it is necessary to establish the linkage between the macroscopic fracture behaviour and micro-morphology. Fig. 9 (a) - (c) shows scanning electron micrographs of fracture surface morphologies for ABS/PET-G (a) (30/70) (b) (50/50) and (c) (70/30) blends. *Post mortem* fracture surfaces always appeared completely stress-whitened indicating micro-void formation and ductile fracture. The shear yielding followed by cavitations predominated in impact tests [35-36]. Fig. 9 (a) of the failure surface of 30/70 ABS/PET-G blend reveals that premature failure occurs because of poor adhesion between phases in neat blends, as indicated by the crack fracture propagating across the interface. The 50/50 blend with fairly good degree of interface adhesion gives supporting evidence for the co-continuity. The ABS/PET-G 70/30 blend has the best toughness with

more voids and cavitations compared with the other samples. Cavitation caused by rubber particles is one of the most important toughening mechanisms. These are plastic deformations resulting from the extensive deformation of material at the fracture surface, enhanced by strong interactions between the phases. In ABS/PET-G (70/30), impact strength is increased considerably. This can be understood from the fracture surface morphology which shows ductile failure with discontinuous stress paths. Here the applied impact energy is fully absorbed by the PET particles. The fracture surface morphology of the neat blends indicated a high extent of debonding, i.e. a lack of adhesion between the phases that aggravates the incompatibility problem as evidenced by the formation of micro voids irrespective of the nature of the dispersed phase (ABS or PET-G). These large debonded domains cannot hinder a propagating crack and premature failure occurs. The poor fracture property of the samples can also be explained by considering the morphology as observed in the SEM. The SEM photograph indicates the presence of large particles distributed haphazardly. The larger particles cannot act effectively in dissipating mechanical energy but instead act as defects [37-38].

3.8. Effect of compatibilization on failure surface morphology

The impact failure surfaces of compatibilized blends are seen Fig. 10 (a)–(c). It is interesting to make a comparison of failure surfaces of these blends with the neat counterpart, in Fig. 10 (c). The multiple fracture paths seen in compatibilized blends, especially at 1% copolymer concentration, as seen in Fig. 10(a) are due to enhanced rubber plastic adhesion. In fact, in such blends yielding of the matrix can be observed. Also, these particles promote and control the impact force by transferring the stresses to the matrix. The compatibilized blends showed high degree of interfacial bonding and no signs of voids could be seen as seen in the figures. This observation is consistent with the earlier results on studies reported by Leclair and Favis [39].

4. CONCLUSIONS

This systematic study was carried out to understand the complex nature of the commercially important compatibilized ABS/PET-G/SBS blends. Morphological characterization of the blends by scanning electron microscopy revealed lack of adhesion between the phases as evidenced by the formation of microvoids irrespective of the nature of the dispersed phase. Over a broad range of composition from 40/60, 50/50 through 60/40, ABS/PET-G blends formed cocontinuous structures, followed by a phase inversion beyond 60 wt. % of PET-G.

These blends are characterized by a two-phase morphology, a narrow interface and poor physical and chemical interactions across the phase boundaries. Stress-transfer characteristics (impact and tensile strengths) of the blends were found to have a strong dependence on the blend ratio. The observed changes in mechanical properties explained on the basis of the fracture surface morphology revealed lack of compatibility as the dispersed domains showed little sign of adhesion to the matrix.

The mechanical property improvement, finer and uniform morphology of compatibilized systems was correlated with the improved interfacial condition of the compatibilized blends. SEM observations prove that SBS acts as a compatibilizer as evidenced by morphology refinement and preferential location at the interface indicating a significant degree of compatibilization. Outstanding mechanical performance, especially improved tensile and impact properties are observed at a critical value of its concentration (CMC). Addition of SBS beyond the saturation level, CMC adversely affected the ultimate properties. The experimental compatibilization results are in agreement with the predictions of Noolandi and Hong. The conformation of the copolymer at the interface was evaluated by characterising the area occupied by the copolymer at the blend interface. The conformation of the compatibilizer molecule at the interface is in between the fully extended and flat configurations as evident from the interfacial area values. Thus, melt processing and compatibilization are very important for development of multiphase polymer materials of ABS/PET-G with well-balanced ultimate properties with a small amount of compatibilizer.

Acknowledgement

Financial support for this research from the Institutional Research Development Programme (IRDP) of the NRF, the University of Pretoria and Xyris Technology CC is gratefully acknowledged.

REFERENCES

1. T. J. Cavanaugh, A. P. Russo and E. B. Nauman, Designing polymer blends, Chem. Tech. 26, 27-32 (1996).
2. A. C. Patel, R. B. Brahmbatt, B. D. Sarawade and S. Devi, Morphological and mechanical properties of PP/ABS blends compatibilized with PP-g-2-HEMA, J. Appl. Polym. Sci. 88, 72-78 (2003).
3. D. R. Paul, in: Polymer blends, D. R. Paul and S. Newman (Ed.) Vol. 2. pp. 5-62. Academic Press, Inc, New York, (1978).

4. N. M. Larocca, E. Hage Jr and L. A. Pessan, Toughening of poly (butylene terephthalate) by AES terpolymer, Polymer 45, 5265-5277(2004).
5. C. H. Tsai and F. C. Chang, Polymer blends of PBT and PP compatibilized by ethylene-co-glycidyl methacrylate copolymers, J. Appl. Polym. Sci. 61, 321-332 (1996).
6. Z. M. Li, X. R. Fu, S. Yang, M. B. Yang, W. Yang and R. Huang, Deformation and morphology development of poly(ethylene terephthalate)/polyethylene and polycarbonate/polyethylene blends with high interfacial contact during elongation, Polym. Eng. Sci. 44, 1561-1570(2004).
7. L. B. Canto, E. Hage Jr. and L. A. Pessan, Effects of the molecular structure of impact modifier and compatibilizer on the toughening of PBT/SBS/PS-GMA blends, J. Appl. Polym. Sci. 102, 5795-5807 (2006).
8. X. Liu, A. Boldizar, M. Rigdahl, H. Bertilsson, Mechanical properties and fracture behaviour of blends of acrylonitrile-butadiene-styrene copolymer and crystalline engineering plastics, J. Appl. Polym. Sci. 86, 2435-2448 (2002).
9. L. B. Brennan, D. H. Isaac and J. C. Arnold, Recycling of acrylonitrile-butadiene-styrene and high-impact polystyrene from waste computer equipment, J. Appl. Polym. Sci. 86, 572-578 (2002).
10. B. Fox, G. Moad, G. V. Deipen, I. Willing, and W. D. Cook, Characterisation of poly(ethylene terephalate) and ABS blends, Polymer 38, 3035-3043(1997).
11. G. Wildes, H. Keskkula and D. R. Paul, Fracture characterization of PC/ABS blends: effect of reactive compatibilization, ABS type and rubber concentration, Polymer 40, 7089-7107 (1999).
12. A. Mamat, T. Vu-Khanh, P. Cigana and B. D. Favis, Impact fracture behaviour of nylon-6/ABS blends, J. Appl. Polym. Sci. Part B. Polym. Phy. 35, 2583-2592 (1999).
13. W. D. Cook, T. Zhang, C. Moad, G. V. Deipen, F. Cser, B. Fox and M. O'Shea, Morphology-property relationships in ABS/PET blends. 1. compositional effects, J. Appl. Polym. Sci. 62, 1699-1709 (1996).
14. M. L. Xue, Y. L. Yu, H. H. Chuah, J. M. Rhee, N. H. Kim and J. H. Lee, Miscibility and compatibilisation of poly(trimethylene terephthalate)/poly(acrylonitrile-butadiene-styrene) blends, Eur. Polym. J. 43 3826-3837 (2007).
15. A. D. T. Gorton and T. D. Pendle, New rapid measurement of crosslink density in compounded natural rubber lattices, NR Technol. 7, 77-81 (1996).
16. P. Jannasch and B. Wesslen, Poly(styrene-graft-ethylene oxide) as a compatibilizer in polystyrene/ polyamide blends, J. Appl. Polym. Sci. 58, 753-770 (2003).

17. S. Wu, Formation of dispersed phase in incompatible polymer blends: Interfacial and rheological effects, Polym. Eng. Sci. 27(5) 335-343 (1987).
18. S. H. Jafari, P. Potschke, M. Stephan, H. Warth, and H Alberts, Multicomponent blends based on polyamide 6 and styrenic polymers: morphology and melt rheology, Polymer 42, 6985-6992 (2002).
19. D. Heikens and W. M. Barentsen, Particle dimensions in polystyrene/polyethylene blends as a function of their melt viscosity and of the concentration of added graft copolymer, Polymer 18, 69-72 (1977).
20. Z. Oommen, B. Kuriakose, C. K. Premaletha and S. Thomas, Melt rheological behaviour of natural rubber/poly(methyl methacrylate)/natural rubber-g-poly (methyl methacrytale)blends, Polymer 23, 5611-5619 (1997).
21. S. Jose, A. S. Aprem, B. Francis, M. C. Chandy, P. Werner, V. Alstaedt and S. Thomas, Phase morphology, crystallization behaviour and mechanical properties of isotactic polypropylene/high density polyethylene blends, Eur. Polym. J. 40, 2105-2115 (2004).
22. J. Huitric, P. M. Médéric Moan and J. Jarrin, Influence of composition and morphology on rheological properties of polyethylene/polyamide blends, Polymer 39, 4849-4856 (1998).
23. X. F. Xu, R. Wang, Z. Y. Tan, H. D. Yang, M. Y. Zhang and H. X. Zhang, Effects of polybutadiene-g-SAN impact modifiers on the morphology and mechanical behaviors of ABS blends, Eur. Polym. J. 41, 1919-1926 (2005).
24. G. I. Taylor, The viscosity of a fluid containing small drops of another fluid, Proc, R., Soc., London, Ser, A138, 41-48 (1932).
25. D. R. Paul in Polymer Blends, D. R Paul and S. Newman, Eds., Academic Press, New York, Chapter 12 (1978).
26. L. Leibler, Theory of phase equilibria in mixtures of copolymers and homopolymers. 2. Interfaces near the consolute point, Macromolecules 15(5) 1283-1290 (1982).
27. J. Noolandi and K. M. Hong, Interfacial properties of immiscible homopolymer blends in the presence of block copolymers, Macromolecules 15(2), 482-492(1982).
28. J. Noolandi and K. M. Hong, Effect of block copolymers at a demixed homopolymer interface, Macromolecules 17(8), 1531-1537(1984).
29. S. Thomas and R. E Prud'homme, Compatibilizing effect of block copolymers in heterogeneous polystyrene/poly (methyl methacrylate) blends, Polymer 33, 4260-4269 (1992).
30. H. Suarez, J. W. Barlow and D. R. Paul, Mechanical properties of ABS/polycarbonate

blends, J. Appl. Polym. Sci. 29, 3253-3259 (1984).
31. S. Joseph, F. Lauprêtre, C. Negrell and S. Thomas, Compatibilising action of random and triblock copolymers of poly (styrene-butadiene) in polystyrene/polybutadiene blends: a study by electron microscopy, solid state NMR spectroscopy and mechanical measurements, Polymer 46, 9385-9395(2005).
32. T. G. Gopakumar, S. Ponrathnama, A. Lele, C. R. Rajan and A. Fradet, In-situ compatibilisation of poly(phenylene sulphide)/wholly aromatic thermotropic liquid crystalline polymer blends by reactive extrusion:morphology, thermal and mechanical properties, Polymer 40, 357-364 (1999).
33. I. Fortelny´, J. Michalkova, J. Hroma´dkova and F. Lednicky, Effect of a styrene-butadiene copolymer on the phase structure and impact strength of polyethylene/high-impact polystyrene blends, J. Appl. Polym. Sci. 81, 570-580 (2001).
34. G. G. Echevarrı´a, J. L. Eguiaza´bal and J. Naza´bal, Influence of compatibilisation on the mechanical behaviour of poly(trimethylene terephthalate)/poly(ethylene-octene) blends, Eur. Polym. J. 43, 1027–1037(2007).
35. K. Cho, J. Wang and C. E. Park, The effect of rubber particle size on toughening behaviour of rubber-modified poly(methyl methacrylate) with different test methods, Polymer 39, 3073-3080(1998).
36. Y. Kayano, H. Keskkula and D. R. Paul, Fracture behaviour of some rubber-toughened nylon-6 blends, Polymer 39, 2835-2845 (1998).
37. A. J. Kinloch, in: Rubber toughened plastics, Advances in Chemistry Series, Washington, pp. 67-91 (1989).
38. G. Levita, in: Rubber toughened plastics, Advances in Chemistry Series, Washington, pp. 93-118. (1989).
39. A. Leclair and B. D. Favis, The role of interfacial modifier in immiscible binary polymer blends and its influence on mechanical properties, Polymer 37, 4723-4728 (1996).

List of Figures

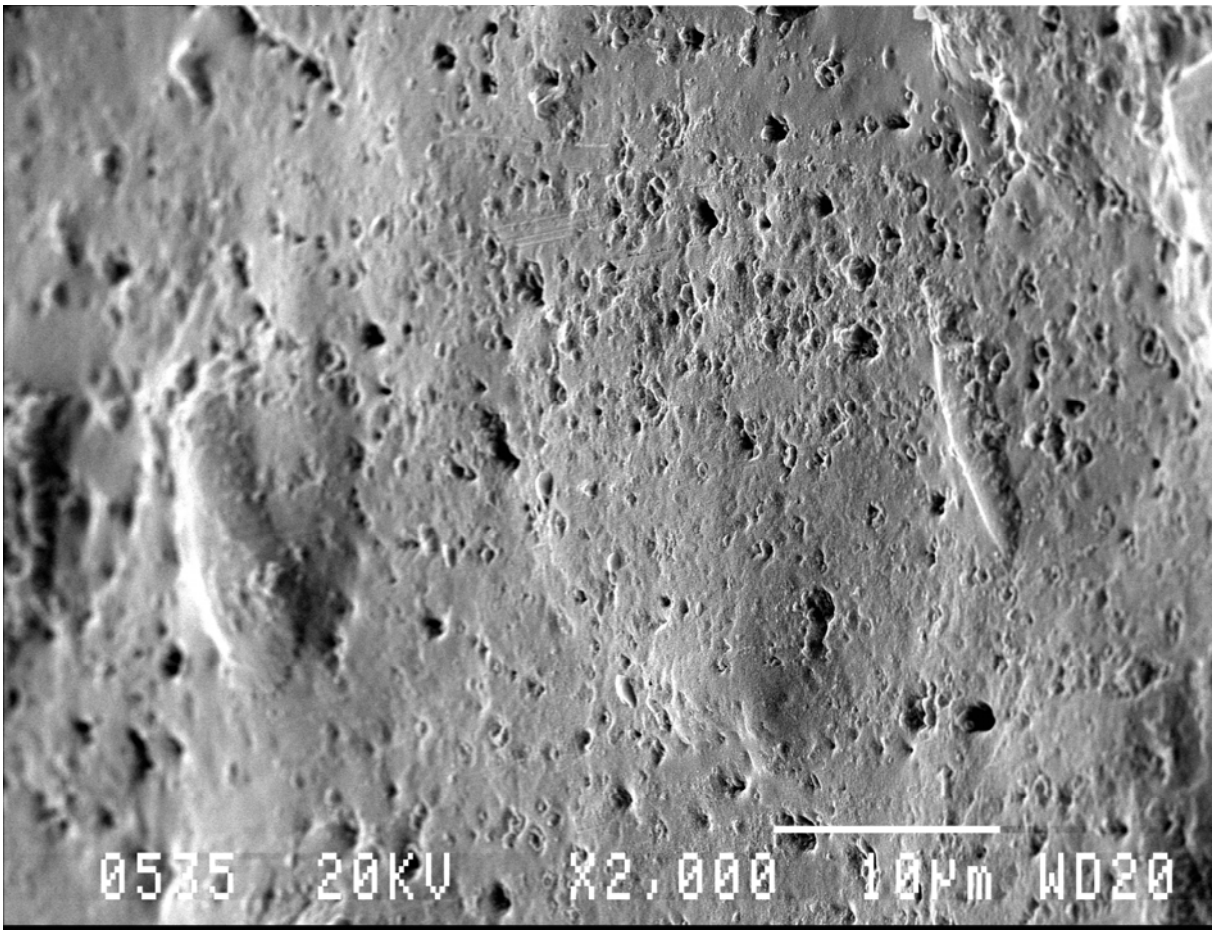

(a)

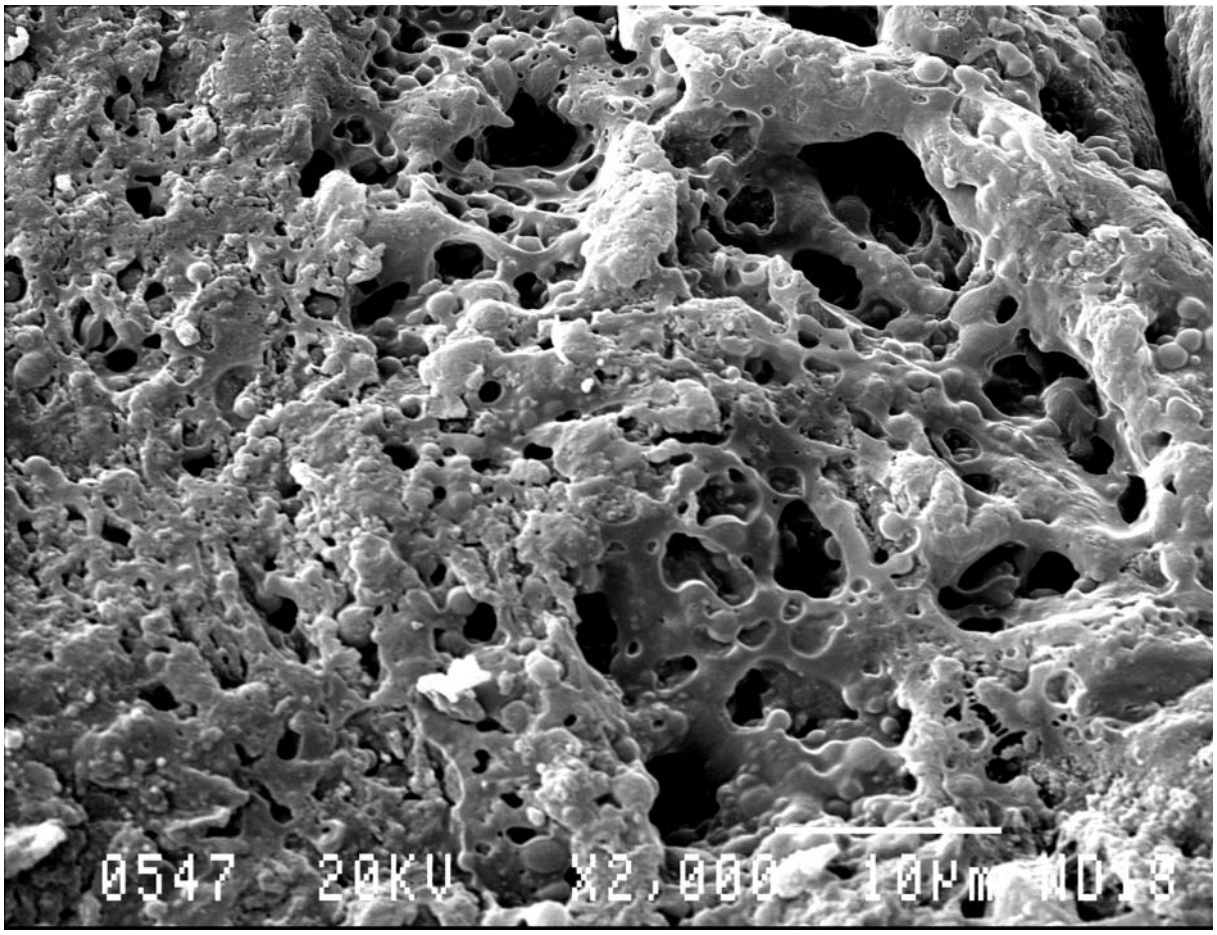

(b)

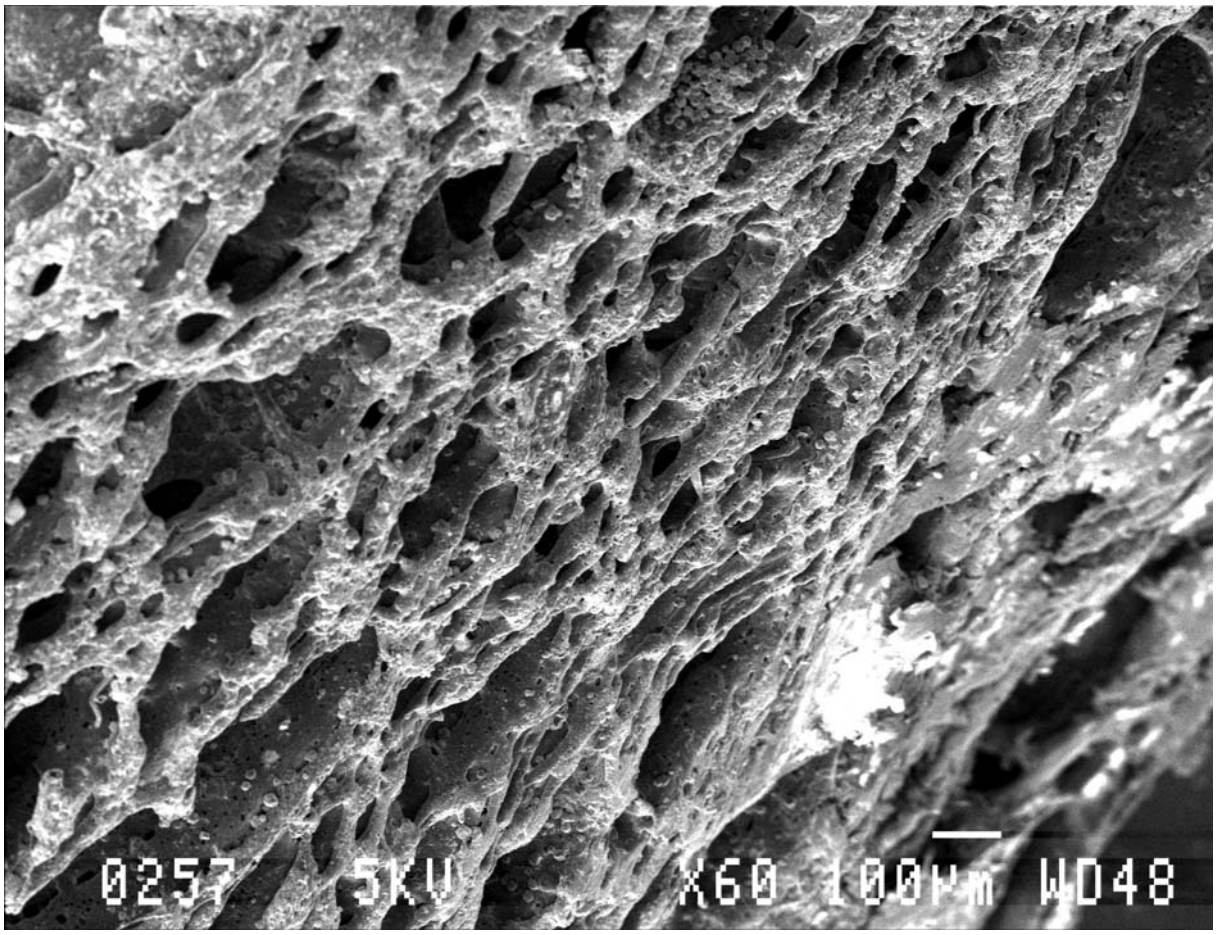

(C)

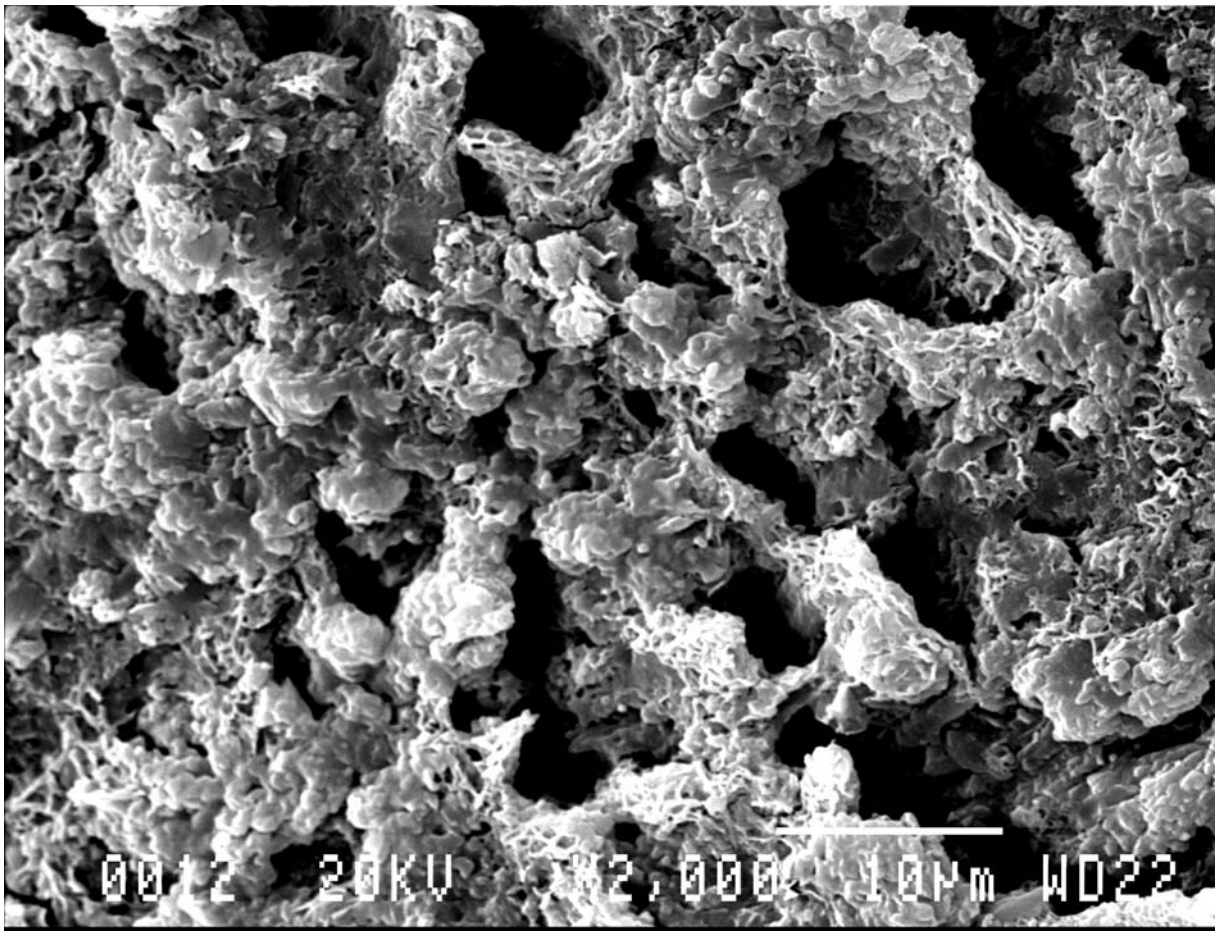

(d)

(e)

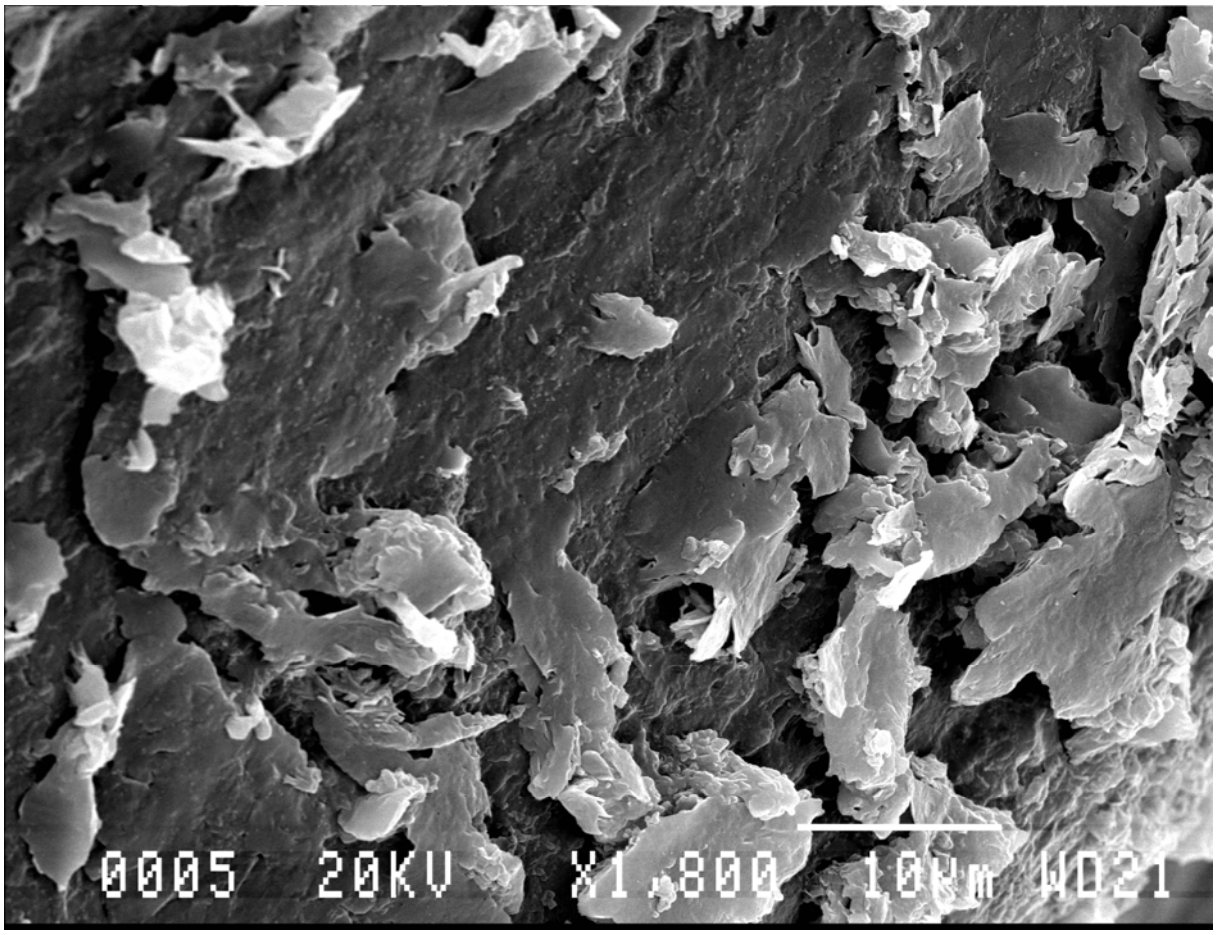

(f)

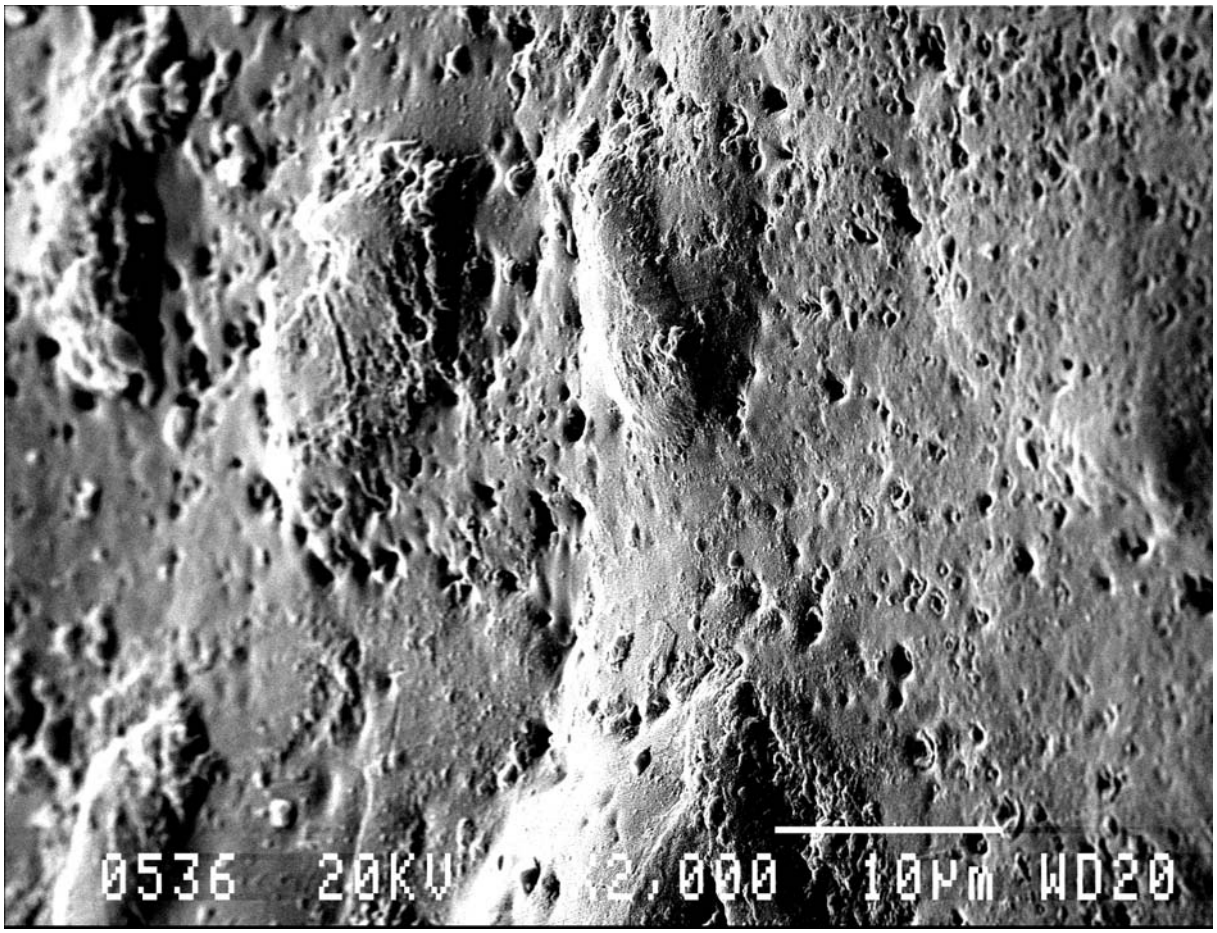

(g)

Figure 1. SEM micrographs showing the morphology of (a) 10/90; (b) 30/70; (c) 40/60; (d) 50/50; (e) 60/40 ;(f) 70/30 ;and (g) 90/10 ABS/PET-G blends.

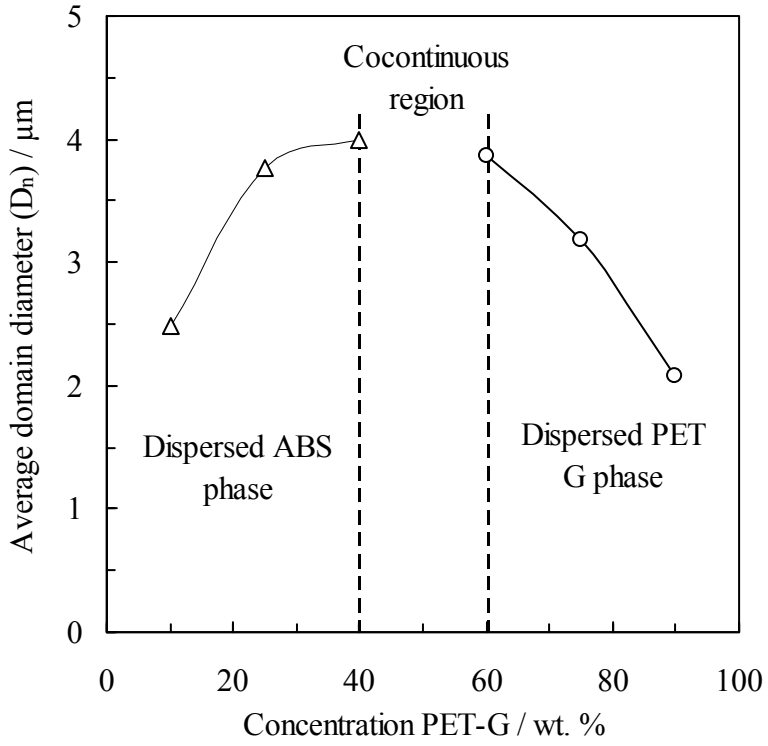

Figure 2. The average particle size of the dispersed phase versus ABS composition.

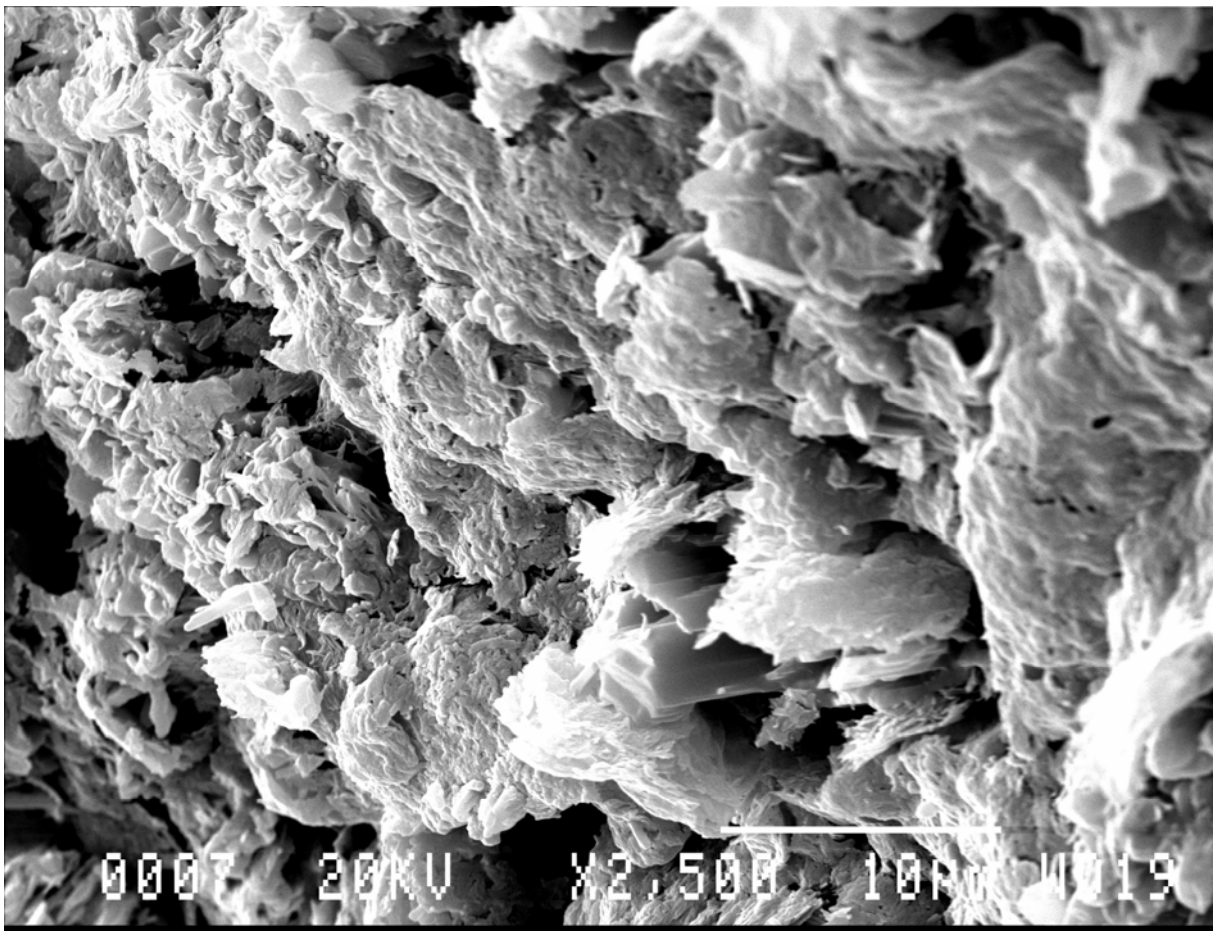

(a)

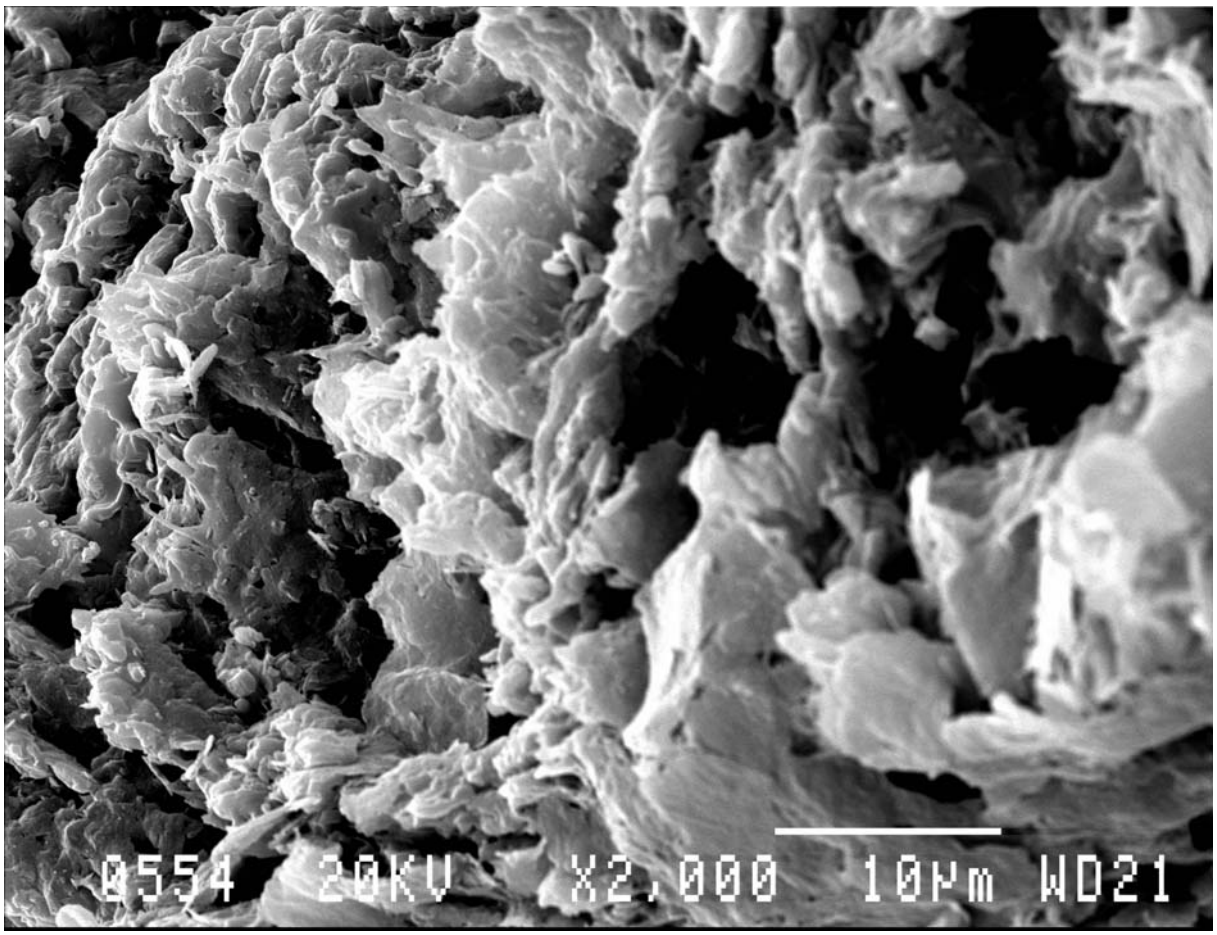

(b)

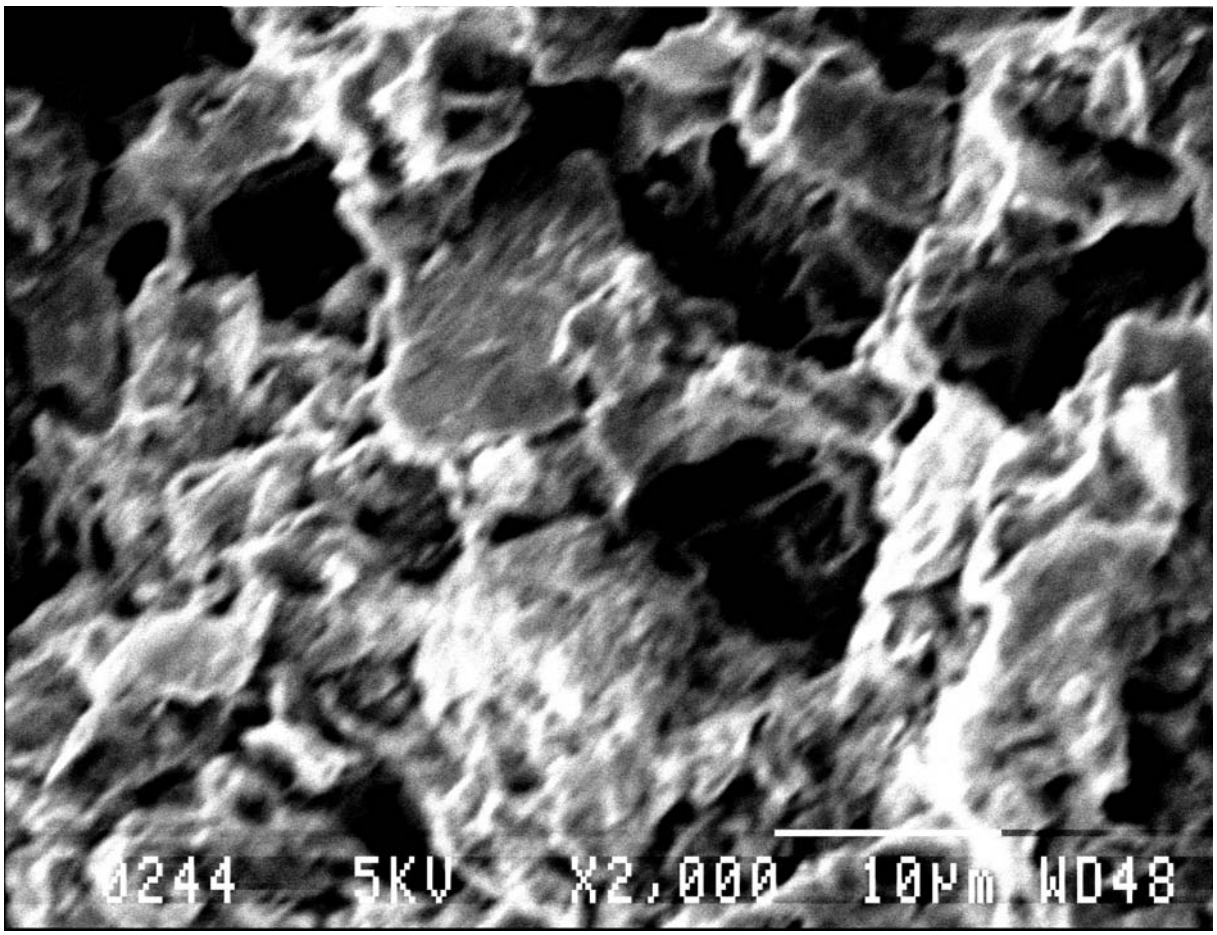

(c)

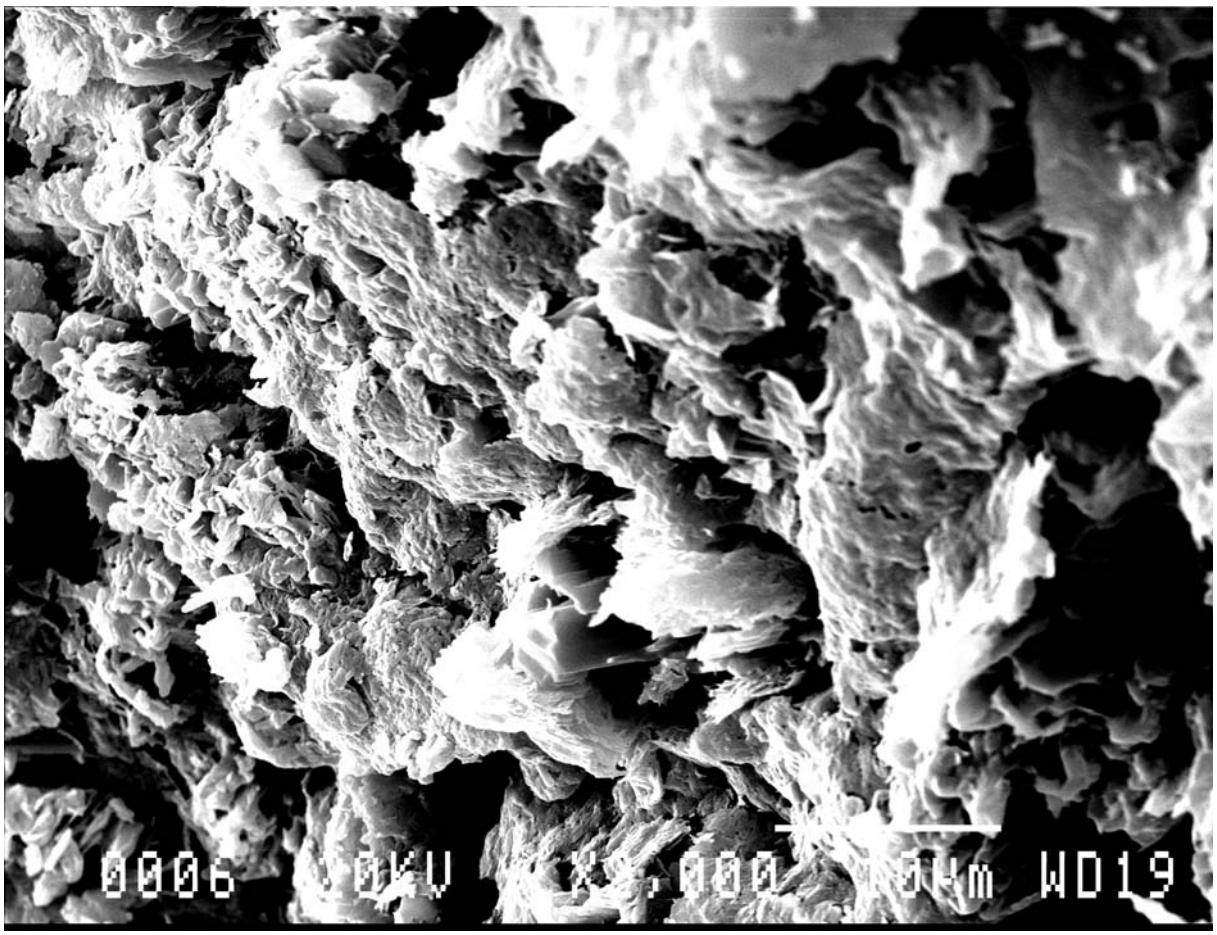

(d)

Figure 3. SEM micrographs of PET-G /ABS blends compatibilized with SBS concentrations (a) 1%; (b) 3%; (c) 5% and (d) 10% respectively.

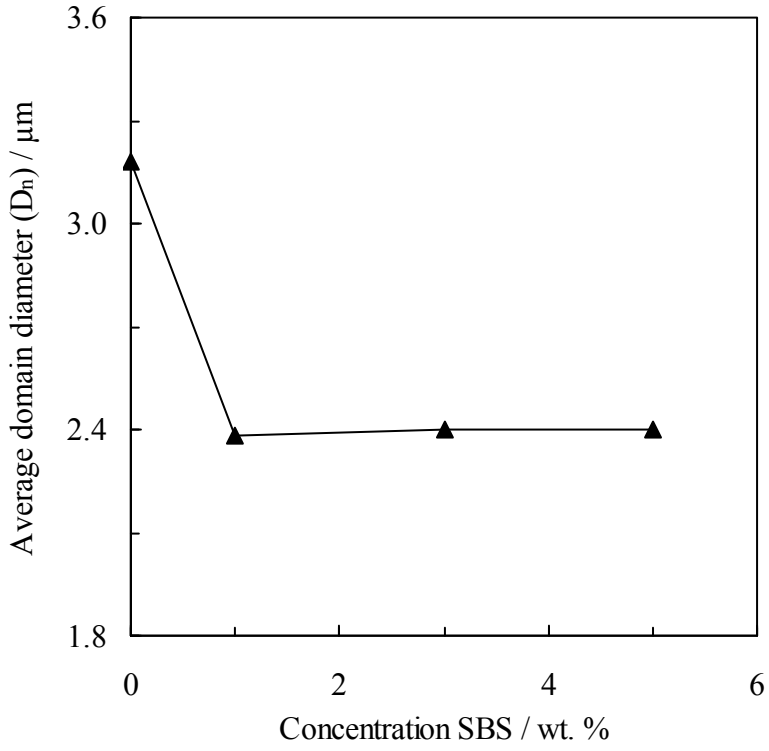

Figure 4. Plot of average domain diameter versus compatibilizer loading for ABS/PET-G (70/30) blends.

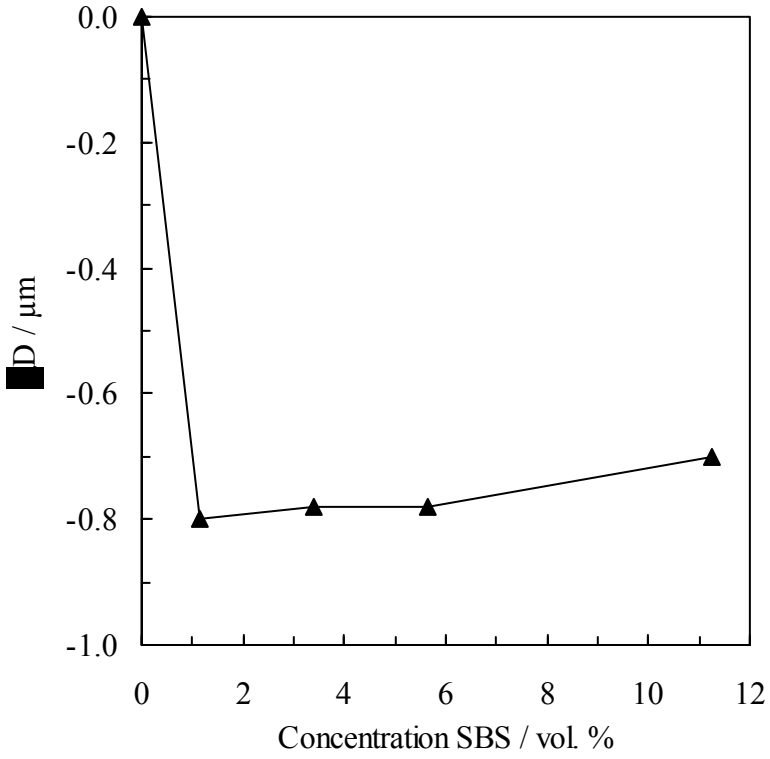

Figure 5. Effect of volume fraction of SBS on the domain size reduction of ABS/PET-G (70/30) blends.

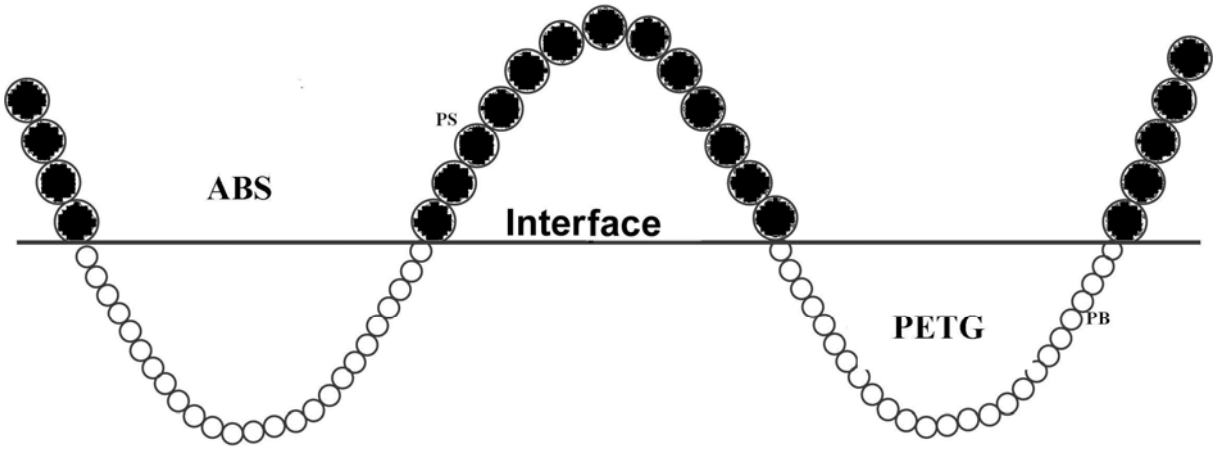

(a)

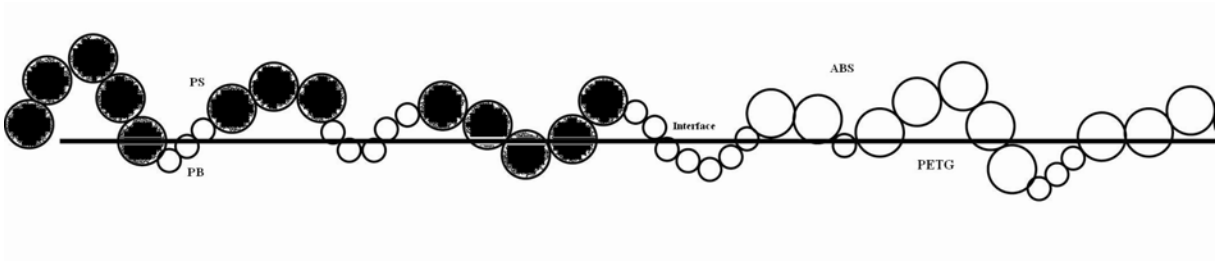

(b)

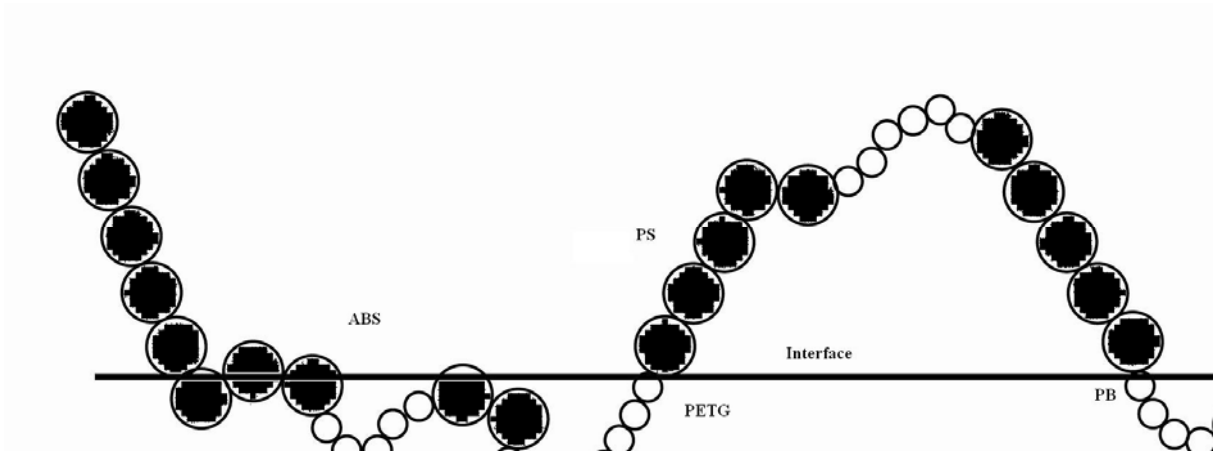

(c)

Figure 6. Different physical models illustrating the conformation of the copolymer at the blend interface (a) fully extended ;(b) completely flat and (c) intermediate.

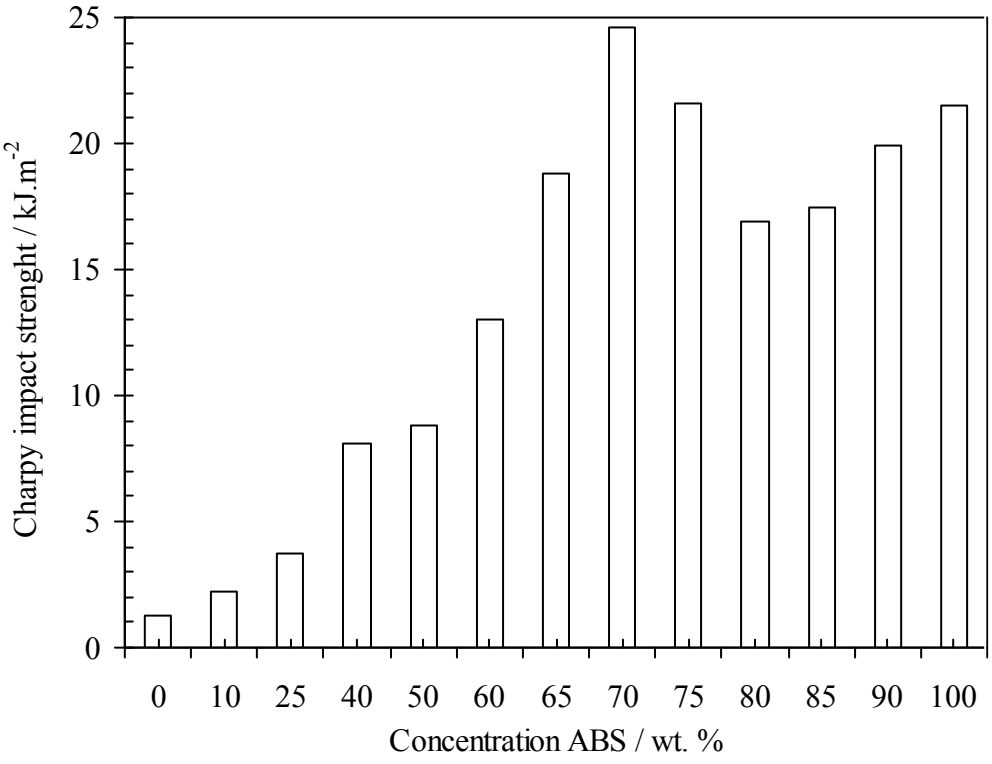

Figure 7. The tensile and impact strength of the blends with ABS content.

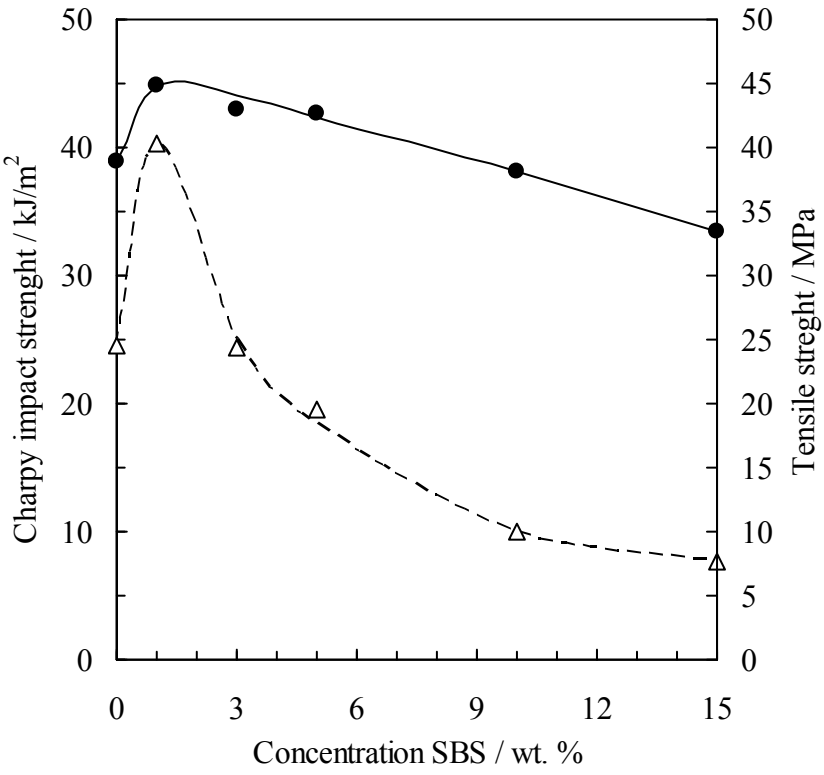

Figure 8. Effect of SBS concentration on the tensile and impact strength of ABS/PET-G (70/30) blends.

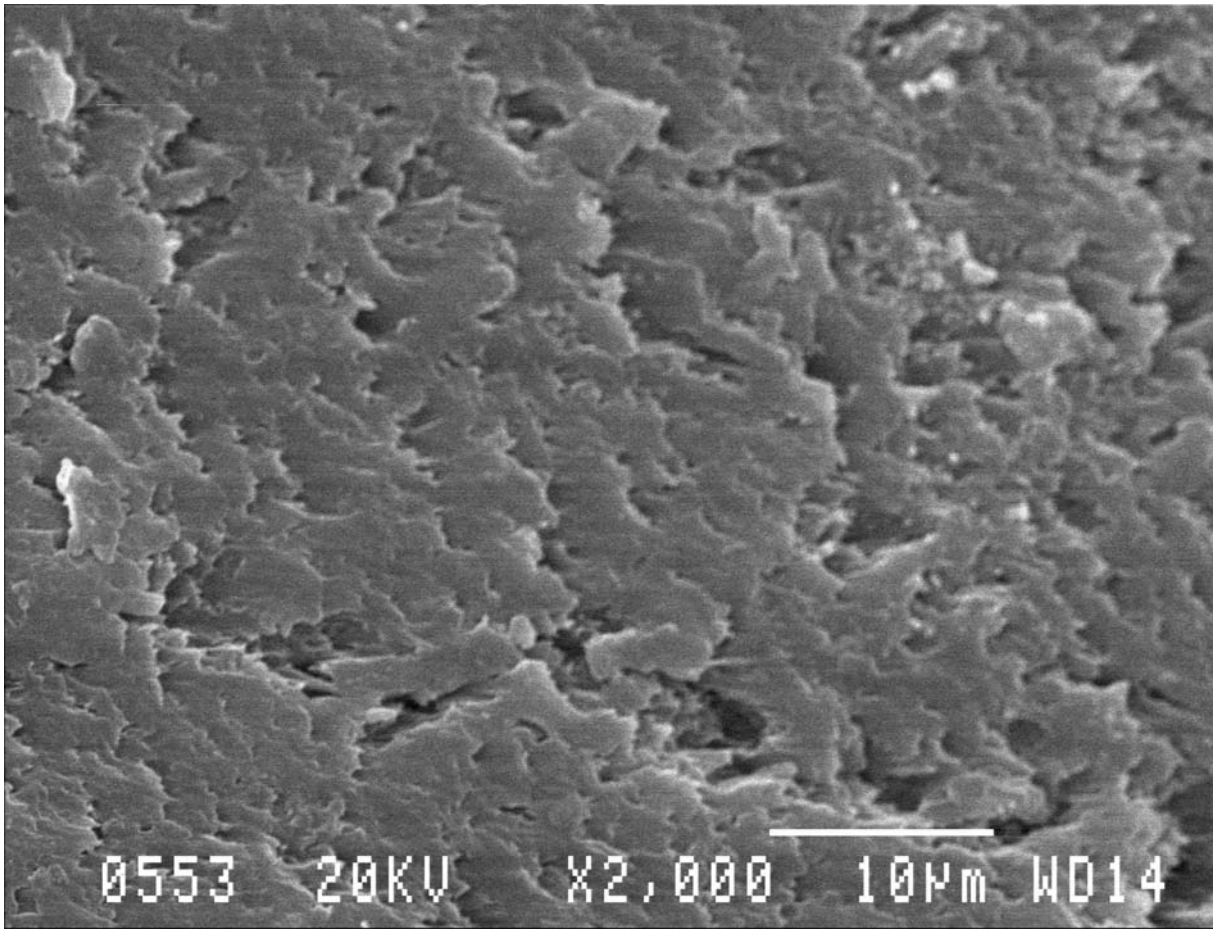

(a)

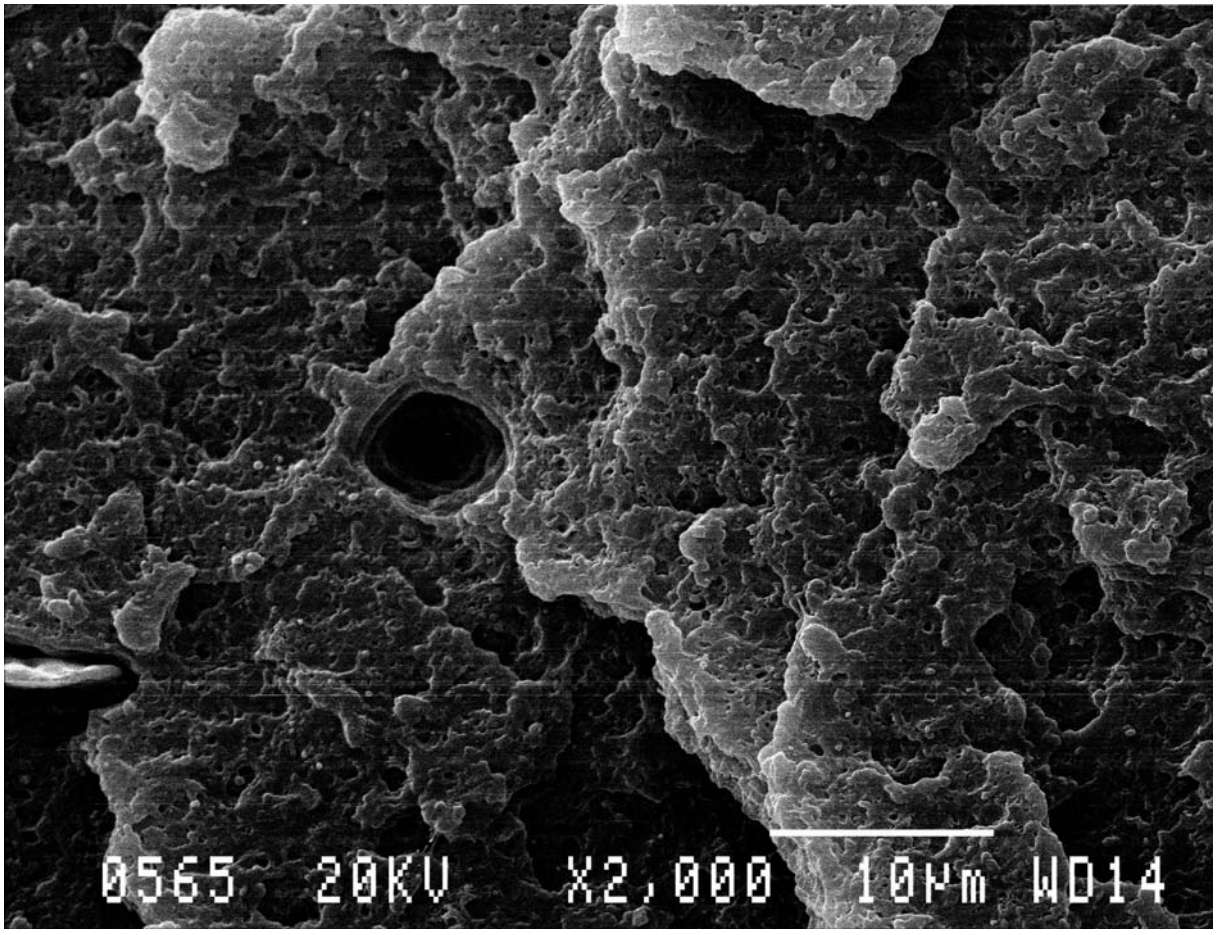

(b)

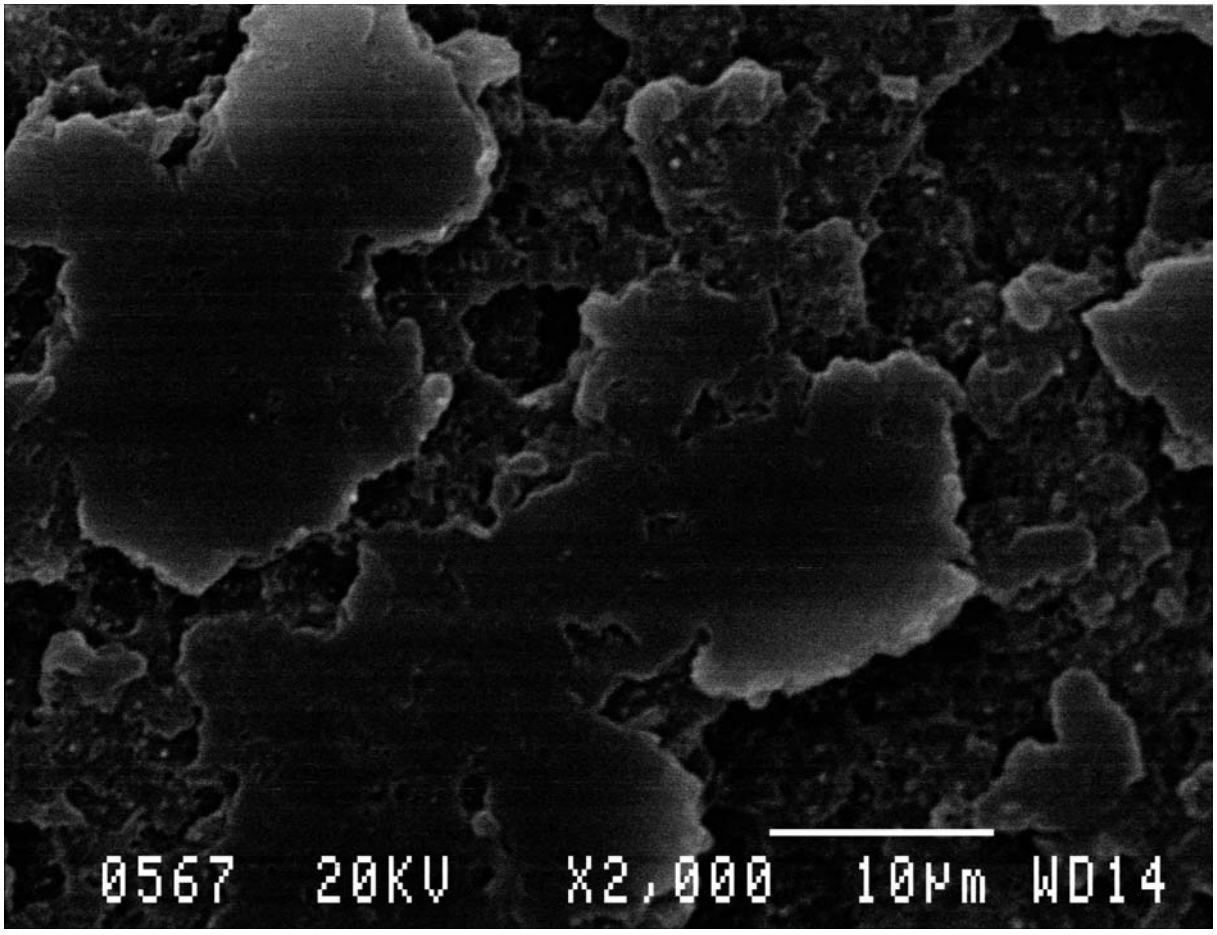

(c)

Figure 9. Scanning electron micrographs showing failure surface morphology (a) (30/70); (b) (50/50); and (c) (70/30) ABS/PET-G blends.

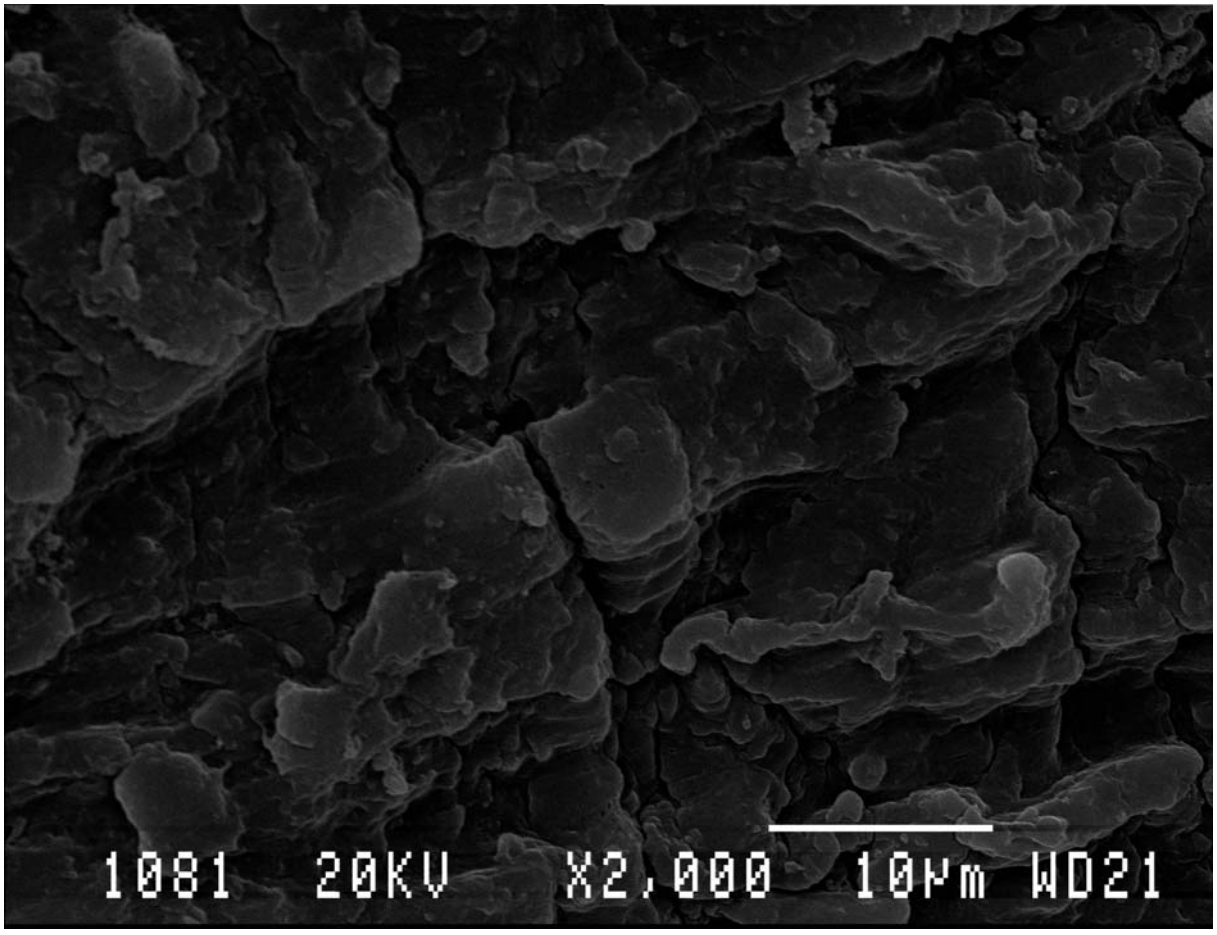

(a)

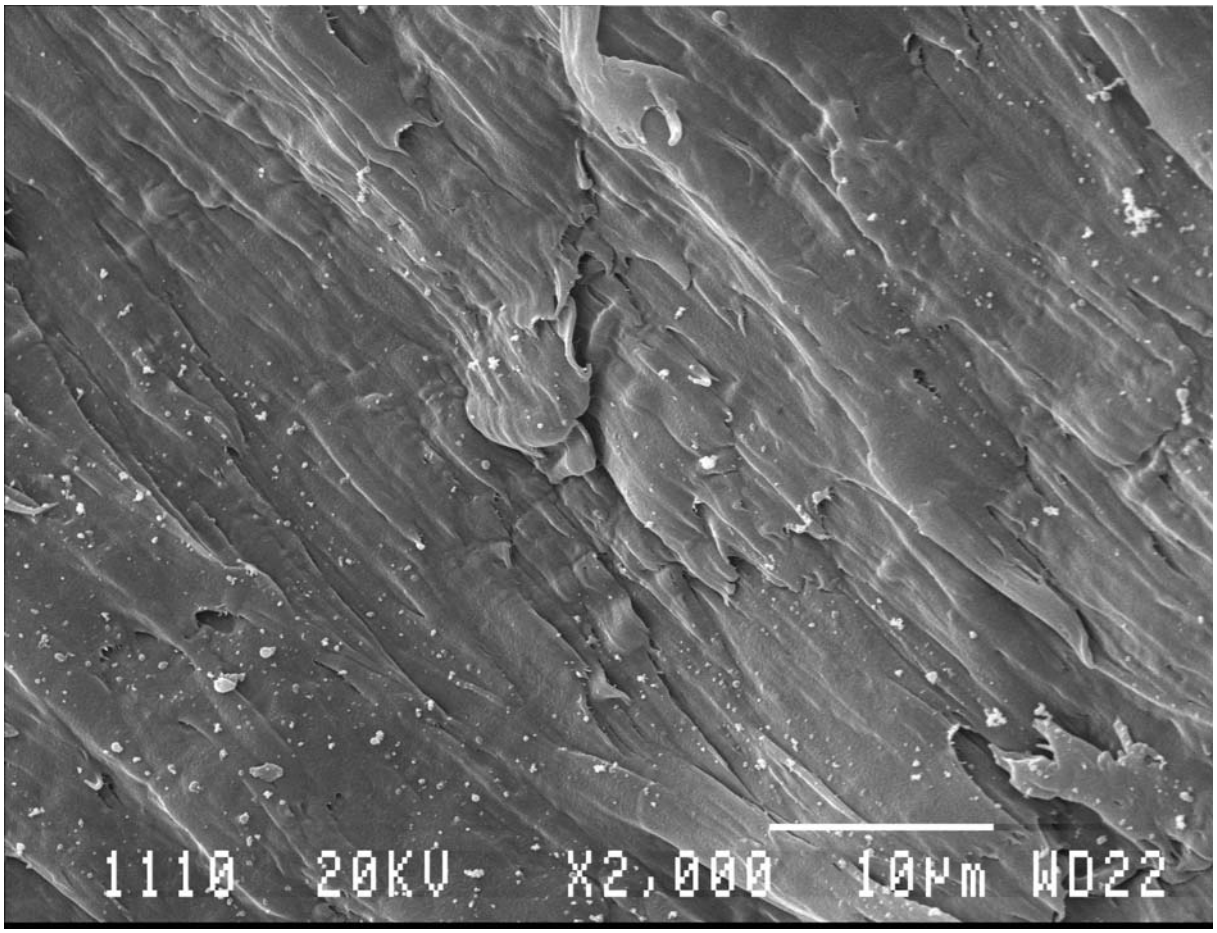

(b)

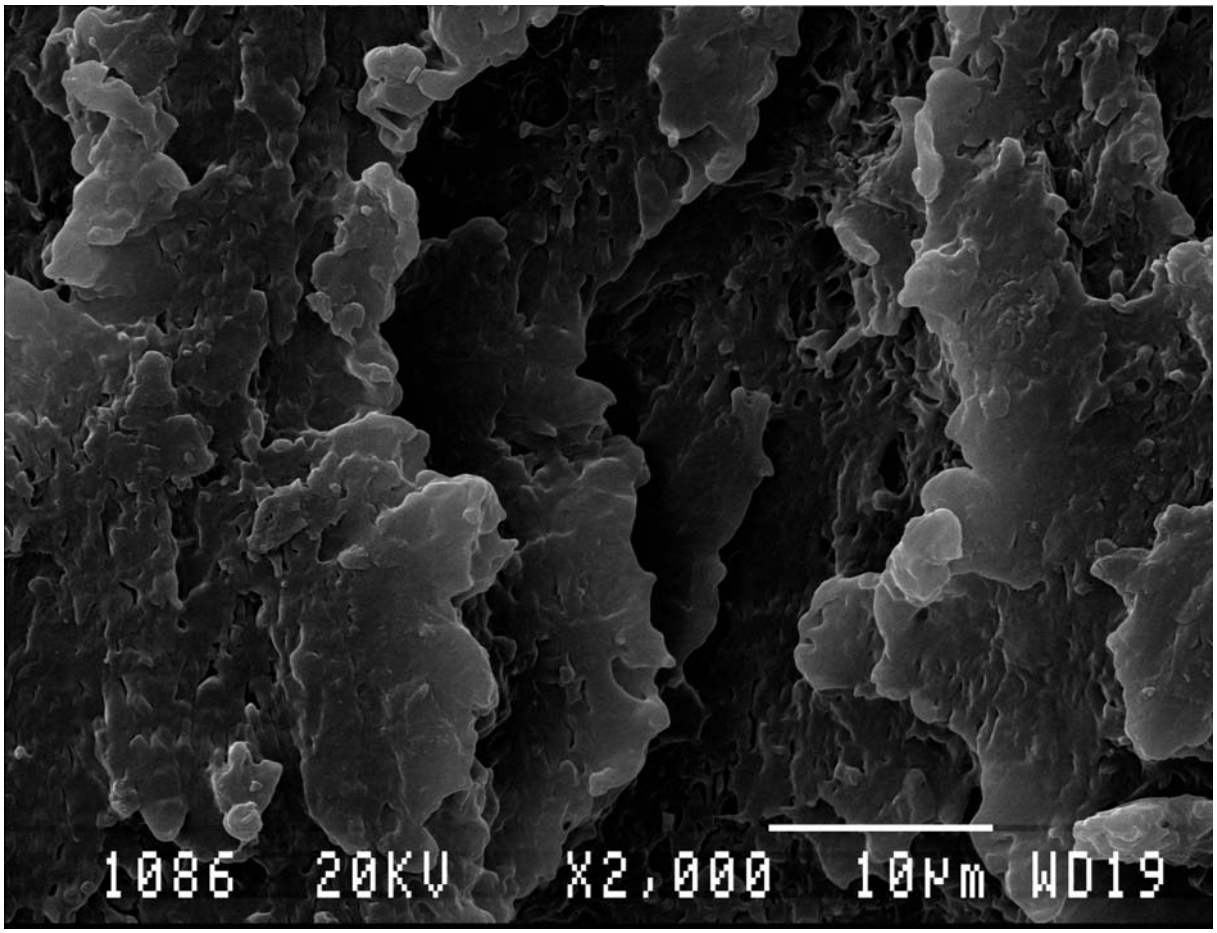

(c)

Figure 10. Scanning electron micrographs showing failure surface morphology of the (70/30) ABS/PET-G blends containing (a) 1; (b) 3; and (c) 5 wt. % SBS.